

AD-A134866

Modeling Study of a cw HF Resonance Transfer Laser Medium

MUNSON A. KWOK and ROGER L. WILKINS

Aerophysics Laboratory
Laboratory Operations
The Aerospace Corporation
El Segundo, Calif. 90245

30 September 1983

Prepared for

AIR FORCE WEAPONS LABORATORY
Kirtland Air Force Base, N. Mex. 87117

APPROVED FOR PUBLIC RELEASE;
DISTRIBUTION UNLIMITED

SPACE DIVISION
AIR FORCE SYSTEMS COMMAND
Los Angeles Air Force Station
P.O. Box 92960, Worldway Postal Center
Los Angeles, Calif. 90009


DTIC
ELECTE
NOV 21 1983
S
E

DTIC FILE COPY

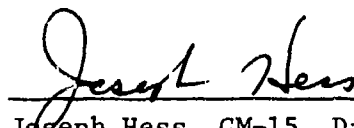
This report was submitted by The Aerospace Corporation, El Segundo, CA 90245, under Contract No. F04701-82-C-0083 with the Space Division, Deputy for Technology, P.O. Box 92960, Worldway Postal Center, Los Angeles, CA 90009. It was reviewed and approved for The Aerospace Corporation by W. P. Thompson, Director, Aerophysics Laboratory. 1st Lt Steven G. Webb, WCO, AFSTC, was the project officer for Technology.

This report has been reviewed by the Public Affairs Office (PAS) and is releasable to the National Technical Information Service (NTIS). At NTIS, it will be available to the general public, including foreign nationals.

This technical report has been reviewed and is approved for publication. Publication of this report does not constitute Air Force approval of the report's findings or conclusions. It is published only for the exchange and stimulation of ideas.



Steven G. Webb, 1st Lt, USAF
Project Officer



Joseph Hess, GM-15, Director
West Coast Office, AF Space Technology
Center

UNCLASSIFIED

SECURITY CLASSIFICATION OF THIS PAGE (When Data Entered)

REPORT DOCUMENTATION PAGE		READ INSTRUCTIONS BEFORE COMPLETING FORM
1. REPORT NUMBER SD-TR-83-59	2. GOVT ACCESSION NO. AD-A134866	3. RECIPIENT'S CATALOG NUMBER
4. TITLE (and Subtitle) MODELING STUDY OF A CW HF RESONANCE TRANSFER LASER MEDIUM		5. TYPE OF REPORT & PERIOD COVERED
7. AUTHOR(s) Munson A. Kwok and Roger L. Wilkins		6. PERFORMING ORG. REPORT NUMBER TR-0083(3603)-3
8. PERFORMING ORGANIZATION NAME AND ADDRESS The Aerospace Corporation El Segundo, California 90245		9. CONTRACT OR GRANT NUMBER(s) F04701-82-C-0083
11. CONTROLLING OFFICE NAME AND ADDRESS Air Force Weapons Laboratory Kirtland Air Force Base, N. Mex. 87117		10. PROGRAM ELEMENT, PROJECT, TASK AREA & WORK UNIT NUMBERS
14. MONITORING AGENCY NAME & ADDRESS (if different from Controlling Office) Space Division Air Force Systems Command Los Angeles, California 90009		12. REPORT DATE 30 September 1983
		13. NUMBER OF PAGES 76
		15. SECURITY CLASS. (of this report) Unclassified
		15a. DECLASSIFICATION/DOWNGRADING SCHEDULE
16. DISTRIBUTION STATEMENT (of this Report) Approved for public release; distribution unlimited		
17. DISTRIBUTION STATEMENT (of the abstract entered in Block 20, if different from Report)		
18. SUPPLEMENTARY NOTES		
19. KEY WORDS (Continue on reverse side if necessary and identify by block number) chemical lasers HF optical resonance transfer laser modeling continuous lasers HF optical resonance transfer lasers HF chemical kinetic modeling hydrogen fluoride chemical kinetics HF chemical kinetics infrared lasers HF continuous chemical lasers lasers		
20. ABSTRACT (Continue on reverse side if necessary and identify by block number) A nonreactive kinetics model of the flowing gaseous medium of a cw HF optical resonance transfer laser (ORTL) has been developed and used to examine the prospects of this type of laser for efficient performance. Model development has required the generation of HF(v ₁ , J ₁) + HF(v ₂ , J ₂) V-V, R-R, T, and V-R cross sections by classical trajectory calculations and by surprisal methods. These cross section packages have been validated using non-ORTL HF kinetics experiments, and the entire ORTL medium model has been validated by modeling		

DD FORM 1473
(FACSIMILE)

UNCLASSIFIED

SECURITY CLASSIFICATION OF THIS PAGE (When Data Entered)

UNCLASSIFIED

SECURITY CLASSIFICATION OF THIS PAGE(When Data Entered)

19. KEY WORDS (Continued)

optical resonance transfer lasers
rotational-to-rotational processes
vibrational-to-vibrational processes

20. ABSTRACT (Continued)

the reported experimental results of past ORTL experiments without any adjustment of the kinetics packages.

The subsequent study observing the effect on small signal gain by varying controllable parameters, such as pumping laser radiative flux and flux distribution, flow velocity, flow density, and HF mole fractions, has suggested a regime for most efficient ORTL operation, in which overall efficiency could reach 0.50. For this regime, pumping laser fluxes should exceed 5000 W/cm^2 with a spectral pattern in which most of the power is in $P_1(5)$, $P_1(6)$, $P_2(5)$, and $P_2(6)$. The medium should be operated at slightly elevated temperatures to enhance kinetic-pumping rates with characteristic velocities allowing any ORTL fluid element to remain in the pump beam no longer than 200 μsec . At that point, V-R processes begin to degrade the gain. A potential problem with gas heating due to the absorption of pump radiation can be nullified by the addition of high specific heat diluents.

(micro)

UNCLASSIFIED

SECURITY CLASSIFICATION OF THIS PAGE(When Data Entered)

PREFACE

This study could not have been performed without the major assistance of Karen L. Foster in programming and computations. We thank George Judd for adapting the NEST program to our problem needs. We appreciate the continuing discussions with Dr. L. Wilson and Dr. D. Drummond of AFWL/ARAC. Finally, we thank Lydia Hammond for typing the manuscript.

Accession For	
NTIS GRA&I	<input checked="" type="checkbox"/>
DTIC TAB	<input type="checkbox"/>
Unannounced	<input type="checkbox"/>
Justification	
By	
Distribution/	
Availability Codes	
Dist	Avail and/or Special
A-1	



CONTENTS

PREFACE	1
1. INTRODUCTION.....	9
2. MODEL DEVELOPMENT.....	11
A. Fundamental Concepts.....	11
B. Collisional Energy Transfer State-to-State Coefficients for HF + M.....	17
C. HF ORTL Model.....	23
3. MODEL VALIDATION AND SIMULATION OF HUGHES ORTL.....	31
A. Number Densities.....	31
B. Static Temperature.....	33
C. Small Signal Gains.....	33
D. Sensitivity of ORTL to Collisional Processes.....	37
4. ORTL MODEL PARAMETRIC STUDIES.....	41
A. Flow Velocity.....	42
B. Pump J-Distribution.....	42
C. Pump Flux Variations.....	48
D. Temperature.....	50
E. Best Regime.....	52
5. CONCLUSION.....	55
REFERENCES.....	59
APPENDICES	
A. Kinetics Equation Listing.....	61
B. Gain and Absorption Coefficients.....	79

FIGURES

1. HF energy level diagram showing an optical resonance pumped transfer laser system.....	13
2. R-R,T endothermic state-to-state rate coefficients for T=300 K predicted using surprisal analysis.....	19
3. ORTL model comparison to the rotational relaxation of Hinch and Hobbs.....	21
4. Excitation of HF(v=1) and HF(v=2).....	24
5. ORTL model schematic with double pass pump laser coupling.....	27
6. Comparison of ORTL model and experiments of ORTL medium HF(v) number densities as a function of HF mole fraction.....	32
7. ORTL medium static temperature as a function of HF mole fraction.....	34
8. Small signal gain coefficients as a function of flow distance X or time t. Initial conditions as shown in Table 6.....	35
9. Small signal gain coefficients as a function of flow distance X or time t. For $X_{HF}=0.01$	38
10. Case as in Fig. 8, but with V-V rate package removed.....	40
11. Small signal gain coefficients as a function of t or X at nearly four-fold slower flow velocity.....	43
12. The dependence of peak gain coefficient on pump flux J distribution.....	45
13. The effect of gas heating on static temperature in the direction of ORTL gas flow with pump flux J distribution as a variable.....	46
14. The shift to higher J in the peak gain $P_{2 \rightarrow 1}(J)$ ORTL transition as pump flux J distribution shifts to higher J.....	47
15. The dependence of peak gain coefficient on total pumping radiative flux.....	49
16. The effect of elevated initial static temperature, 700 K, on $P_{2 \rightarrow 1}(J)$ small signal gain coefficients.....	51

TABLES

1.	ORTL Size.....	15
2.	Rughe HF ORTL.....	16
3.	HF + M Collision Processes $v < 2$, $J < 15$	20
4.	Comparison of Measured and Model Transfer Rates.....	22
5.	Comparison of Quenching Coefficients at $T=300$ K for the HF(v_1) + HF($v_2=0$) System.....	25
6.	ORTL Input Parameters.....	30
7.	Observed Lasing Compared to Model Gain Coefficient.....	36
8.	Increase in ORTL Medium Heat Capacity.....	52

1. INTRODUCTION

The cw Optical Resonance (pumped) (collisional) Transfer Laser (ORTL) has been proposed as a device for improving high power lasers operating at HF or DF wavelengths. These lasers have been studied experimentally by Wang et al.¹⁻⁶ In optical resonance transfer lasers, photon energy from a high flux optical source is resonantly absorbed on vibrational-rotational transitions by a passive, nonreacting, molecular gas. A population in the upper state is rapidly created. Collisional steps follow to access the part of the internal energy manifold in the excited molecule favorable to population inversions and high gain.

The ORTL device is unique in that Wang et al. have concentrated on HF or DF as the optical acceptor of pumping photon flux. They have introduced the idea that the lasing molecular species need not be the same as that of the optical acceptor if rapid collisional transfer exists. They have consequently invented many new laser devices. They have also found that the HF (or DF) ORTL, in which the acceptor and lasing species are the same, has a potential for high overall efficiency. Namely, a large fraction of the photon flux from a pumping HF laser can be converted efficiently into HF ORTL power. This potential high efficiency combines with features attractive to chemical laser systems. Properties conducive to better beam quality performance include pre-mixed operation, laminar subsonic flow, and ORTL lasing on predominantly one vibrational-rotational transition under Wang's conditions of demonstration. As one attractive feature, the ORTL medium is recyclable.

The object of this report is to examine the crucial issue of HF ORTL efficiency prospects under reasonable conditions of operation. These conditions may differ markedly from those of the laboratory demonstrations. The focus will be on the applicability of ORTL as a beam improvement device for an HF high power laser system. It should be stressed that the results and conclusions in this report will not necessarily apply to DF ORTLs, or to medium and low power applications of the concept.

The performance of the ORTL medium depends on a detailed understanding of the individual collisional transfer mechanisms involving $\text{HF}(v_1, J_1) + \text{HF}(v_2, J_2)$ energy transfer on a channel-by-channel basis. This is because the pump radiation is quite state specific on such an $\text{HF}(v, J)$ basis. In one sense, this current study is then an extension of the previous kinetic studies of Wilkins and Kwok,⁷⁻⁸ in which aspects of these classes of laser mechanisms have been closely examined theoretically and experimentally and in which code simulations of past experimental studies have been conducted using the appropriate developed kinetic rate data. The objective of these code studies has always been the improvement of vital cross section data needed for laser modeling.

In Section 2, the ORTL model code development will be described, including validations of the listed rotational-rotational (R-R) and vibrational-vibrational (V-V) kinetics packages by comparisons with selected non-ORTL experimental results. In Section 3, the simulation of the reported² ORTL medium is presented as a further illustration of our model validations. Successful comparisons of HF number densities, static temperature, and zero-power gains are made. The important relative contributions of V-V and R-R transfer in the production of inversions are also examined in Section 3. In Section 4, we carry out parametric studies comparing various regimes of HF pumping laser flux distributions while varying medium initial conditions. For reasons of code simplicity and economy, our principal diagnostic in these sections will be the small signal gain computations. Parametric regimes suitable for an ORTL medium as well as the limitations of the concept as a high power HF device are discussed. The conclusions are summarized in Section 5.

2. MODEL DEVELOPMENT

In subsection A, we will discuss some fundamental concepts needed for an understanding of an HF (or DF) ORTL. Central to our studies is the collisional energy transfer processes in the ORTL. The state-to-state rate coefficients computed by Wilkins for use in the modeling will be briefly summarized in subsection B. In subsection C we will provide a description of the HF ORTL model.

A. FUNDAMENTAL CONCEPTS

A cw HF ORTL system consists of the following elements:

- a. Source of pumping laser radiation
- b. Premixed medium (He/HF) in transverse flow
- c. Mirror structure for coupling the pumped laser into the medium
- d. ORTL resonator and beam extractor
- e. ORTL gas handling systems

An important feature of an HF ORTL medium with no chemical reaction is that the same active HF molecules can be used more than once (recycled) within the mirror structure of the pumped laser. The effective number of cycles has significant influence on the overall ORTL efficiency. From a system viewpoint, the reusability of the exhaust gases appears attractive.

This model describes aspects of the first three listed elements of an ORTL system. The model predictions, which will be compared to experimental results, are small signal gains of selected spectral lines, HF(v,J) number densities, and medium static temperatures for appropriate spatial locations. The advantage of a model, of course, is to enable us to make excursions economically in choices of parameters that are difficult to execute experimentally in a short time.

The current version of the model will not fully assess the effects of recycling. However, evidence for that behavior will be seen in our computations and supporting analysis. To fully simulate the effects on power

extraction from the medium and from recycling, one needs, at least, a laser model with Fabry-Perot mirrors.

1. THE ORTL CYCLE

An HF energy level diagram is shown in Fig. 1 describing the (v, J) levels of the molecules in the ground electronic state. HF molecules are raised from the $v = 0$ state by the resonance absorption of $P_{1,0}(J)$ photons from the pumping laser. The HF($v = 1, J$) molecules can then be excited to the $v = 2$ state by a second resonance absorption of $P_{2,1}(J)$ laser photons from the pump laser or by the following V-V collisional energy transfer process:



Successful ORTL operation requires that lasing occurs at wavelengths longer than those of the pumping transitions. A partial inversion with a significant gain must be developed. In the steady state under proper conditions, the ORTL transitions being optically pumped should be nearly saturated without appreciable gain. The collisional de-excitation of molecules to lower J levels (or shorter wavelength regimes) leads to other HF transitions with absorption. These transitions would tend to have populations in the lower state larger than those in the upper state because of the inclination of the medium toward rotational equilibrium. The collisional excitations of molecules to high J states occur as a result of V-V processes [Eq. (R1)] or rotational-rotational, transitional (R-R,T) transfer processes [(Eq. (R2)] or combinations of both types:



At higher J , the partial inversion has the best chance to develop. The cross sections for collision channels represented by Eqs. (R1) and (R2) should be large for an efficient ORTL.

After ORTL stimulated emission has occurred, the HF molecule must be recycled to (v, J) states where optical or collisional pumping can again

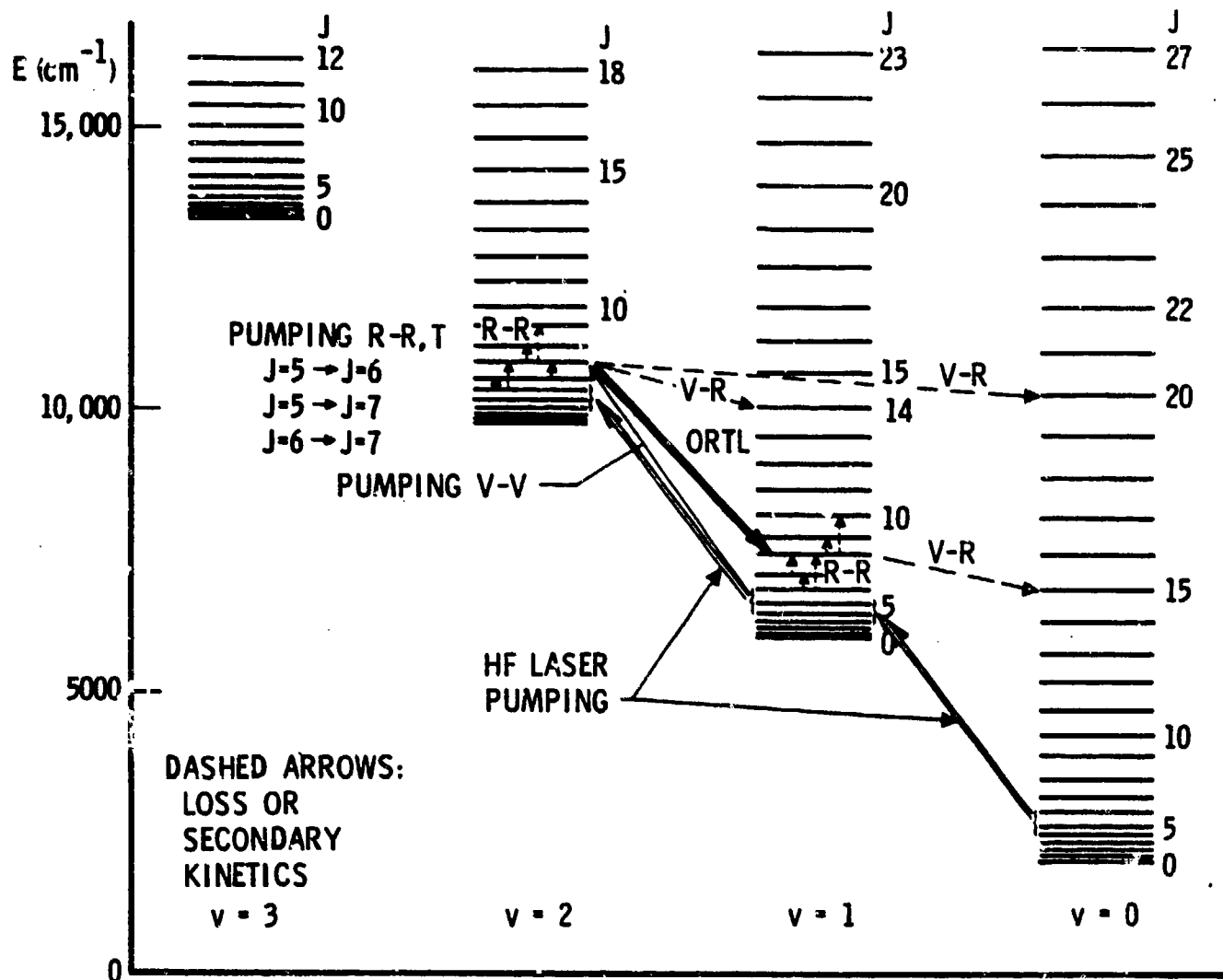
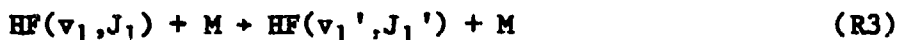


Fig. 1. HF energy level diagram showing an optical resonance pumped transfer laser system.

occur. Important channels for this behavior are the backward reactions of Eq. (R2) and perhaps the backward reactions of Eq. (R1) if the $v = 1$ state is involved after the ORTL lasing on the $P_2(J)$ transition. The R-R,T processes are favored since they are exothermic.

The backward processes of Eqs. (R1) and (R2) can also be construed to be loss mechanisms affecting the efficiency of the ORTL lasing transitions if they influence the populations of the upper states. Other secondary state-scrambling or loss mechanisms might be V-V processes involving $v_1 = 1$ and $v_2 = 2$ (or $v_1 = 2$ and $v_2 = 2$) and V-R,T processes:



where

$M = HF(v_2, J_2)$, diluents

and

$$v_1 - v_1' = +1, 2, \dots, v_1$$

The V-R,T processes will generally be too slow to be of great importance in an ORTL cycle. In contrast, these mechanisms would be quite noticeable in a chemical laser description.

Ideally, pumping flux rates and collisional rates should be sufficiently large so that one characteristic cycling time is considerably less than the time for an ORTL fluid element to pass through the flux fields of the pumping laser.

2. DEFINITIONS OF EFFICIENCIES

Three efficiencies have been defined to describe ORTL performance.² The ORTL input efficiency is:

$$\eta_1 = \frac{\text{power absorbed by ORTL medium}}{\text{incident pump power}} \quad (R1)$$

This quantity is highly dependent on the optical thickness of the transitions in the medium absorbing the pump laser lines. The power conversion efficiency is:

$$\eta_c = \frac{\text{coherent ORTL power}}{\text{power absorbed by ORTL medium}} \quad (\text{E2})$$

and the outcoupling efficiency is

$$\eta_o = \frac{\text{outcoupled ORTL power}}{\text{coherent ORTL power}} \quad (\text{E3})$$

The overall efficiency is

$$\eta_T \equiv \eta_i \times \eta_c \times \eta_o \quad (\text{E4})$$

3. THE SIZE OF AN ORTL DEVICE

An estimate of the size of an ORTL device compared to that of a chemical laser device can be made by assuming a steady state condition and an input efficiency η_i of unity. For a hypothetical chemical laser at 1000 W and stated values of the laser power per unit area of the nozzle face, δ , and the specific power, σ , Table 1 presents estimates for the minimum required HF

Table 1. ORTL Size

Chemical Laser (1 kW)		ORTL (80 Torr, 0.05 HF Fraction)		
			1 cycle	100 cycles
Photon flux (sec^{-1})	1.5×10^{22}	HF flux(sec^{-1})	1.5×10^{22}	1.5×10^{20}
δ (W/cm^2)	50			
σ ($\text{kW sec}/\text{kg}$)	300			
\dot{m} (gm/sec)	2.5	\dot{m}_{total} (gm/sec)	2.5	0.025
v (cm/sec)	10^5	V (cm/sec)	10^3	10^3
A (cm^2)	20	A (cm^2)	125	1.3

flowrate, total mass flowrates, velocities, and nozzle size for both the pump chemical laser and the ORTL. It is also assumed that the ORTL is operating at 80 Torr with a 0.05 HF mole fraction and a 0.95 He mole fraction.

Table 1 illustrates that for an average 100 recycles of ORTL HF molecules within the pump laser flux, the ORTL nozzle will be about the same size as that of a chemical laser nozzle. By this thinking, an increase in the number of effective cycles will correspondingly reduce the ORTL nozzle size and the flow requirements compared to the pump laser.

The overall efficiency η_T of ORTL will typically be less than 0.50 so that in this situation, only about half the power will be produced. On the other hand, the operation of ORTL at high pressures makes the exhaust recovery problem much easier.

A similar examination of size of the ORTL system reported by Hughes yields the data in Table 2.

Table 2. Hughes HF ORTL

Chemical Laser (0.8 kW)		ORTL (80 Torr, 0.05 HF Fraction)	
Photon flux (sec^{-1})	1.2×10^{22}	HF flux (sec^{-1})	$< 1.2 \times 10^{21}$
\dot{m} (gm/sec) nom.	5	\dot{m} (gm/sec)	0.2
V (cm/sec)	$\sim 10^5$	V	5×10^3
A (cm^2) nominal	10	A (cm^2)	1.8

It is apparent that a recycling chain on the order of 1-10 must be operating when the fluxes are compared. Input efficiencies as high as 0.35 were reported by the experimentalists; therefore, the number of cycles is around three at best. For the approximate 0.38 cm width of the laser beam in the direction of

ORTL flow at this ORTL velocity V , the single cycle time is on the order of 20 μsec . The comparison of the pump laser nozzle exit area with that of the ORTL is somewhat misleading because the σ of the pump laser is not high.

For Hughes' operating condition, estimates can be made of the characteristic time for radiative and collisional processes. These can then be compared to the so-called cycle time. Typically, the pump laser flux I_{ph} on a single spectral line is 200 W/cm^2 and the radiative cross section σ_{rad} on the absorbing line is $5 \times 10^{-17} \text{ cm}^2$. The characteristic time τ_{rad} (for radiative pumping) is then

$$\tau_{rad} = \left(\frac{\tau_{rad} I_{ph}}{h\nu} \right)^{-1} \sim 7 \times 10^{-6} \text{ sec}$$

Single channel V-V or R-R,T collision processes will have cross sections ranging from one to five collisions in probability. At pressures of HF at 4 Torr,

$$\tau_{coll} = (k_{coll} N_{HF})^{-1} \sim 0.25-1.2 \times 10^{-6} \text{ sec}$$

Characteristic times for ORTL lasing would be on the order of cavity lifetimes—submicroseconds. It seems clear that the limiting process of an ORTL cycle in this experiment was the radiative pumping process because the photon fluxes were too low.

B. COLLISIONAL ENERGY TRANSFER STATE-TO-STATE RATE COEFFICIENTS FOR HF + M

The state-to-state rate coefficients used in the model have come from two basic calculations: the classical trajectory studies by Wilkins⁹ and recent computations by Wilkins¹⁰ using the surprisal analysis approach. To date, there are no known measured absolute cross sections on single channel HF(v,J) + M processes which include some knowledge of the product (v,J) states. This

degree of refinement is necessary in the modeling of an optically pumped medium in which the pumping fluxes excite very specific (v,J) states. To validate the computed state-to-state rate coefficients, the best available experiments were modeled using versions of the ORTL model code. Some comparison with experiments is, of course, necessary to determine the surprisal parameters when using the information theoretic technique.

A full listing of the kinetic equations used is given in Appendix A. The details of state-to-state rate coefficients computed by the surprisal analyses approach and their applications to modeling will be the subject of another paper.¹⁰

Some indications of the complexity of the kinetics are summarized in Table 3 where the types of $HF(v_1,J_1) + HF(v_2,J_2)$ processes are described. The number of channels possible for each type of process is also given. For the simple V-V energy transfer processes represented by $HF(v=1) + HF(v=1) \rightarrow HF(v=2) + HF(v=0)$, an astonishing number of channels is possible when all possible initial and final J states less than 15 are considered for near-resonant conditions $|\Delta E| < 400 \text{ cm}^{-1}$. To render the ORTL model manageable, we eventually limited the channels listed to $|\Delta E| < 100 \text{ cm}^{-1}$. The subtleties of the many channels of the V-V type of process would seem to be extremely important in an ORTL medium model since the rate coefficient of each channel is typically quite large. There are fewer specific channels for the R-R,T processes, but they are also extremely important for particular ranges of J because the rate coefficients are also quite large [order of $(10^{14} \text{ cm}^3/\text{mol}^{-1}\text{sec}^{-1})$].

To properly write equations for V-R,T processes some product J values greater than 15 were considered.

In Fig. 2, the R-R,T endothermic state-to-state rate coefficients are plotted as a function of initial J for $v = 1$, $J'-J = +1$ through $+5$. The wide range of values for the coefficients can be seen. Implicitly, one can see that there is a limitation to pumping very high J levels in an ORTL medium because the rates become too slow.

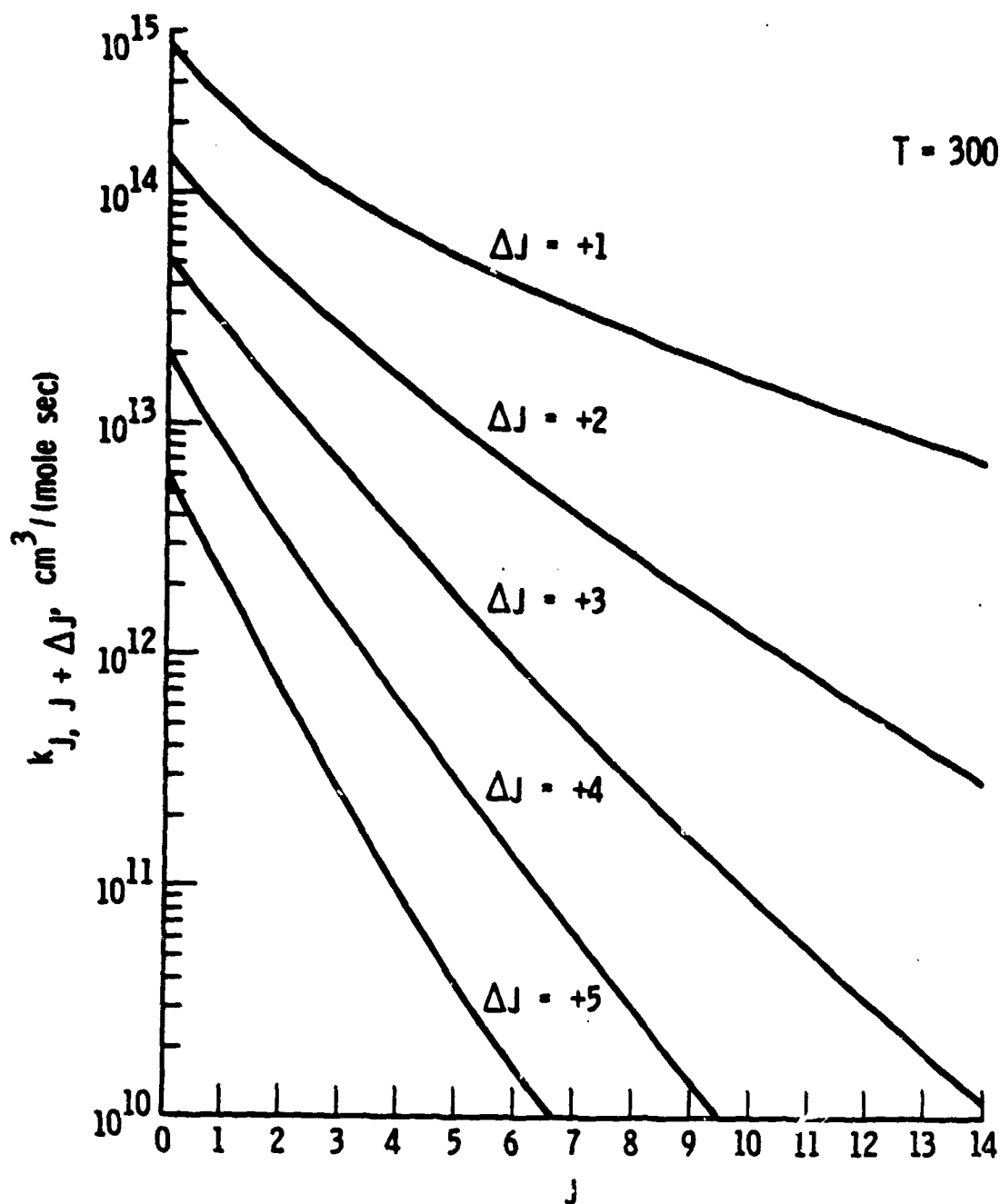


Fig. 2. R-R,T endothermic state-to-state rate coefficients for T=300 K predicted using surprisal analysis.

Table 3. HF + M Collision Processes $v < 2$, $J < 15$

Type	Equation Type	Channels	Order k
R-R, T	$HF(v_1, J_1) + HF(v_2, J_2) \rightarrow HF(v_1', J_1') + HF(v_2', J_2')$		$\text{cm}^3/(\text{mol sec})$
	$J_1' - J_1 = \pm 1, \pm 2, \pm 3, \pm 4$	225	10^{14}
V-V	$HF(v_1=1, J_1) + HF(v_2=1, J_1)$ $\rightarrow HF(v_1'=0, J_1') + HF(v_2'=2, J_1')$, $ \Delta E < 500\text{cm}^{-1}$	30000	$10^{13} - 10^{14}$
V-V	$ \Delta E < 100\text{cm}^{-1}$	426	
V-R, T	$HF(v_1, J_1) + HF(v_2, J_2) \rightarrow HF(v_1', J_1') + HF(v_2, J_2)$	340	10^{12}

1. VALIDATION OF R-R, T STATE-TO-STATE RATE COEFFICIENTS

The validation of the R-R, T state-to-state coefficients is performed by simulating the experimental results of Hinchey and Hobbs,^{11,12} in which an $HF(v_1=1, J_1)$ state was excited by photon pumping from a short pulse HF laser. The subsequent collisional excitation of neighboring $HF(v_2=1, J_2)$ levels was carefully observed by them. Using the kinetic equations developed for the ORTL model, we initially placed an amount of $HF(v, J)$ population out of Boltzmann equilibrium into an $HF(v=1, J)$ state. The density was determined with the aid of reported pulsed laser properties in a manner similar to that to be discussed later. The results are shown in Fig. 3 for the case in which the photolytically pumped state is $HF(v=1, J=3)$. These results are further summarized in Table 4. It can be seen that our kinetic simulation is quite good for $J'-J = \pm 1, \pm 2$, and ± 3 over a range of photolytically pumped initial states. The agreement for $J'-J = 4$ is not as successful. These slower rates, however, are not as important in an ORTL simulation. Details of this work will be given later in another paper.¹³

2. VALIDATION OF V-V STATE-TO-STATE RATE COEFFICIENTS

The V-V state-to-state rate coefficients have been validated by simulating the experimental techniques reported in the works of Osgood, Sackett, and Javan¹⁴ and Bina and Jones.¹⁵ Neither are really highly sensitive tests

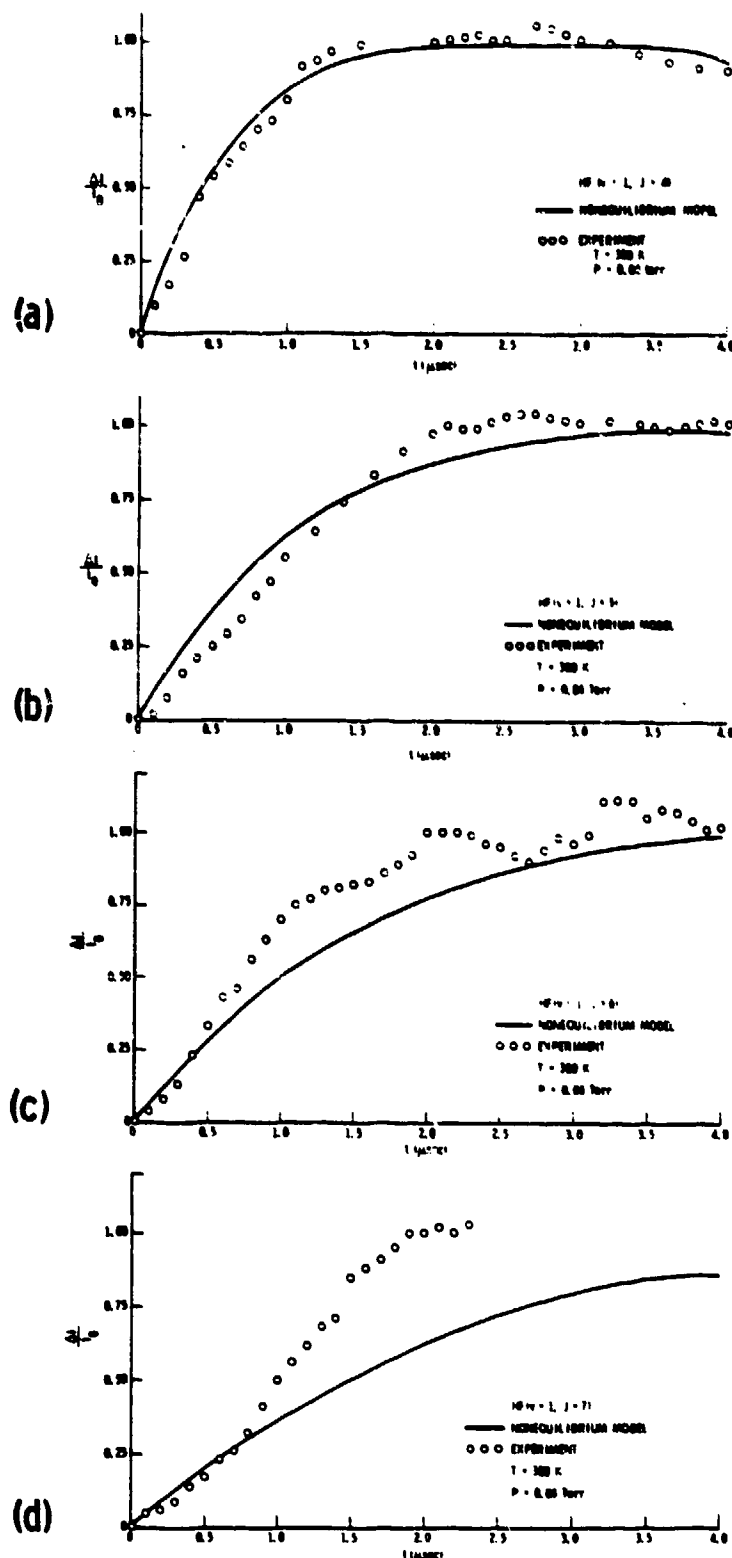


Fig. 3. ORTL model comparison to the rotational relaxation of Hinch and Hobbs. Photolytic pumping of $HF(v=1, J=3)$ by HF pulse lasers. Relative intensities of (a) $HF(v=1, J=4)$; (b) $HF(v=1, J=5)$, (c) $HF(v=1, J=6)$, and (d) $HF(v=1, J=7)$ are shown as a function of time.

Table 4. Comparison of Measured^a and Model^b Transfer Rates

Pump J	Probe J	$1/T_{1J}$ ($\times 10^6 \text{ sec}^{-1} \text{ Torr}^{-1}$) (Measured)	$1/T_{1J}$ ($\times 10^6 \text{ sec}^{-1} \text{ Torr}^{-1}$) Model
2	3	105.	39.
2	4	51.	26.
2	5	27.	13.
2	6	19.	11.
3	4	48.	42.
3	5	24.	25.
3	6	19.	18.
3	7	17.	13.
4	5	58.	48.
4	6	34.	31.
4	7	31.	24.
4	8	10.	19.
5	6	68.	54.
5	7	33.	37.

^aHinchen and Hobbs¹¹

^bInverse power law with $\gamma=0.8$

of the rate scheme since the results of the former study have already been synthesized by us with a much less detailed scheme, and the latter work was really preliminary. Nevertheless, the V-V kinetics are sufficiently successful in duplicating all the reported quantitative features, as shown in Figs. 4a and 4b for the two experiments with quite different initial conditions. Figure 4a shows the growth and decay of $\text{HF}(v=2)$ as reported in the Osgood et al. work with the decay being twice that of $\text{HF}(v=1)$. Bina and Jones reported two decay regimes, as shown in Fig. 4b, with the slower $\text{HF}(v=2)$ decay being twice that of $\text{HF}(v=1)$. A large number of experimental results can be compared with our theoretical results in Table 5. In these experiments it was not possible to separate the V-V and V-R,T parts of the empirical quenching $\text{HF}(v) + \text{HF}(v_2=0)$.

C. HF ORTL MODEL

The HF ORTL model is built upon the NEST code¹⁶, which handles nonequilibrium chemistry problems with one dependent variable, time t or distance x . The original code provided for photolytic excitation as a function of time by selected species in a fixed optical volume. The code accounted for the energy input by the photon flux into the gas volume, but it did not provide information on the spatial variation of the flux within that volume as a result of optical thickness. The need to study individual $\text{HF}(v,J)$ states required a significant expansion of the NEST code and the photolytic excitation or "flashlamp" option. Crucial to the ORTL simulation is a consistent expression of the interaction of laser radiation with the gaseous HF species within the context of the code's flashlamp option. This development is described below.

1. CODE EXPANSION

For this work an expanded version of NEST, designated NESTE, has been developed. The version includes the capability to handle 1100 kinetic equations, 125 species, and the appearance of a species in 250 equations. It also can handle eight flashlamps (or laser lines). Recently the code has been further upgraded to 2000 equations and 16 flashlamps. This additional capability would provide an opportunity to study more complex ORTL systems, such as the cw DF ORTL. The flashlamp option has also been modified to accept

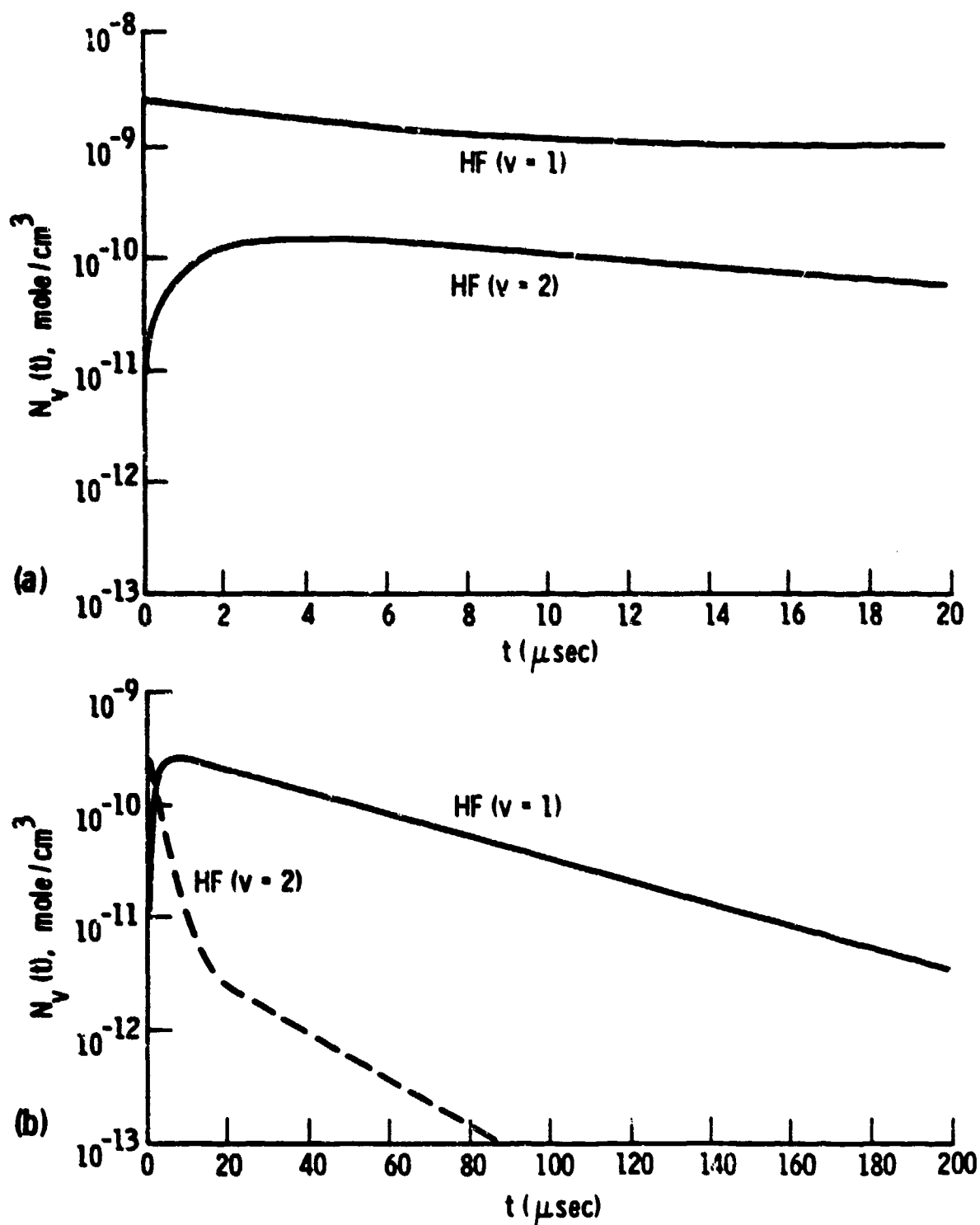


Fig. 4. (a) Excitation of HF($v=1$) and HF($v=2$) by the HF pulse laser pumping of HF($v=1$) and V-V transfer to HF($v=2$). (b) Excitation of HF($v=2$) by direct pulse laser pumping.

Table 5. Comparison of Quenching Coefficients at T=300 K for the $HP(v_1) + HP(v_2=0)$ System^a

$k_{HP}(v), 10^{12} \text{cm}^3/\text{mole sec}$						
$v = 1$	2	3	4	5	6	References
<u>EXPERIMENTS</u>						
1.	16.0 9.9	31.0 15.7	28.0 16.3			Osgood, Sackett, and Javan ¹⁴ Kwok and Wilkins ¹⁸
		11.0		35.0	61.0	Kwok and Cohen ²⁰
	7.8	11.4	19.3	27.7	31.3	Poole and Smith ²¹
		16.9	43.4			Douglas and Moore ²²
1.1	9.6 11.0	12.0	>32.0	>48.0		Bott ²³ Airey and Smith ²⁴ Bina and Jones ¹⁵
		18.1 19.3	44.0 53.0	91.0		Jursich and Grim ²⁵ Lampert, Jursich, and Grim ²⁶
<u>THEORY</u>						
0.49	3.9 13.3	6.0 14.5	11.4 12.0	16.3 7.8	25.9	Billing and Eguilsen ²⁷ Shin and Kim ²⁸
1.1	13.3	12.7	13.3	19.3		Clendening et al. ²⁹
<u>THIS MODEL^b</u>						
1.0	13.4	17.5	19.9	25.1	30.8	

^aThese rate coefficients represent the decay rates resulting from both $v \rightarrow w$ and $v \rightarrow R$ energy-transfer processes.

^bThis model simulates the OSJ technique¹⁴ of sequential photon absorption.

analytical functions as a function of t or x . These include sinusoidal functions, square or rectangular functions, the Gaussian function, and step functions.

2. ORTL MODEL

The ORTL model describes the changes in the ORTL medium as a function of x , the direction of subsonic flow. As a simple one-dimensional flow the transformation between x and t involves U , a defined velocity of the flow,

$$t = \frac{x}{U}$$

The model is schematically illustrated in Fig. 5. It has been assumed that the ORTL medium is a constant area, constant velocity flow. Necessarily in a one-dimensional flow, this medium has a constant density as a function of x . Changes in the gasdynamic parameters of this flow are not great because of the large amount of diluent employed.

The initial conditions of the medium are static pressure, p , static temperature, T , average velocity, U , gas composition of the i^{th} species (He and HF) α_i , and dimensions $d \times W$ of the flow cross section. The initial conditions for photon excitation include the spatial and spectral line distributions of the pump laser fluxes as well as the absolute values of that power distribution.

For the current work, the rectangular flux profile with dimensions a and b will be used. The coupling of the pump laser into the ORTL medium includes, in these cases, a double pass configuration, as shown in Fig. 5. The one-pass interaction length is L .

The important ORTL model outputs as a function of x include:

1. gain coefficient at the spectral line center of HF $2 \rightarrow 1$ and $1 \rightarrow 0$ P-branch lines
2. HF(v, J) number densities
3. static temperature
4. static pressure
5. Voigt line shape and parameters.

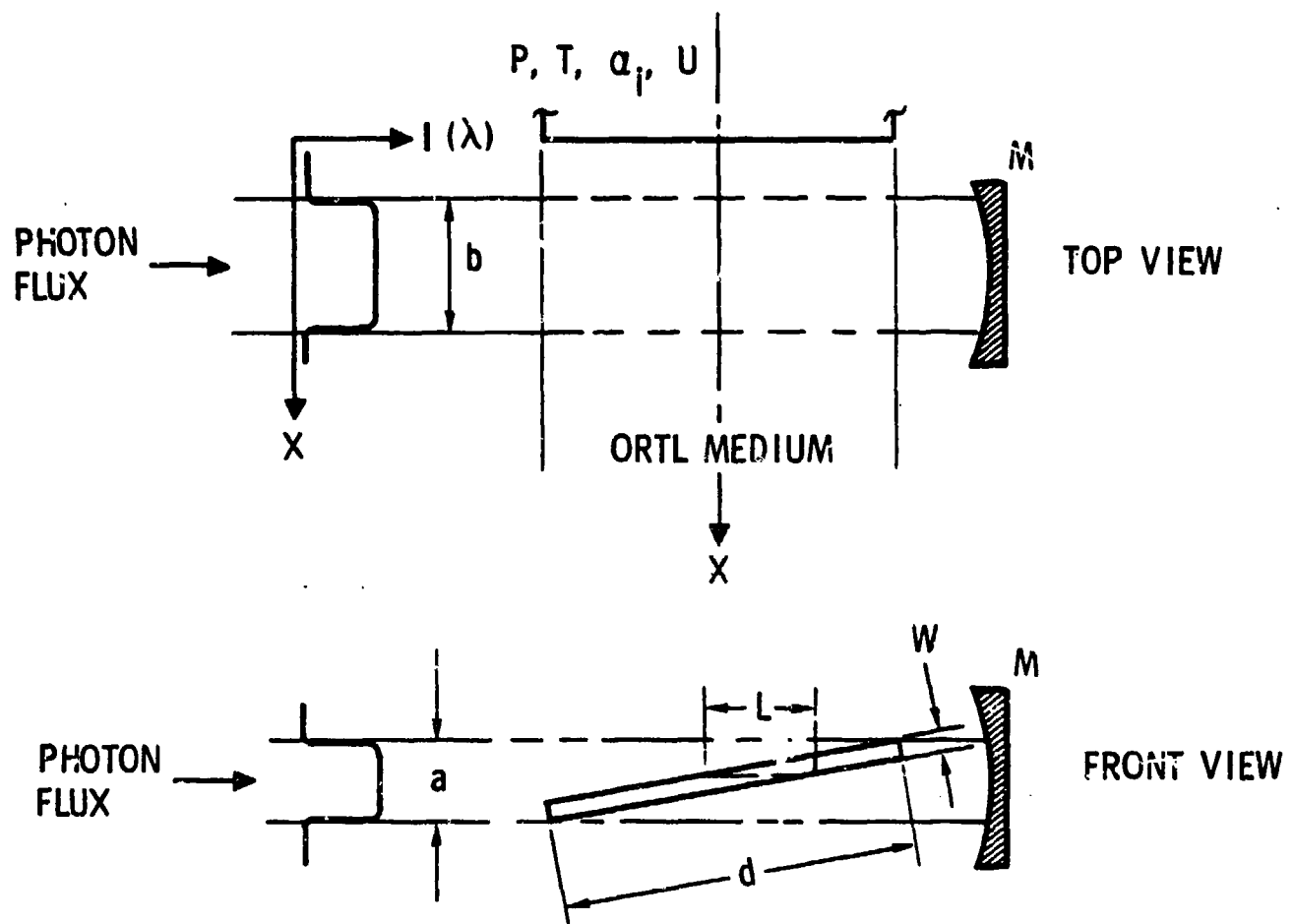


Fig. 5. ORTL model schematic with double pass pump laser coupling.

There are conventional NEST code outputs of secondary importance to this problem. The formulation of the gain coefficient and line-shape expressions are summarized in Appendix 2.

3. INTERACTION OF RADIATION WITH MATTER

Some discussion dealing with resonance absorption within the spectral line is necessary in entering the proper initial conditions for the photolytic excitation. It can be assumed that the pump laser is homogeneously broadened;¹⁷ then the lasing mode of the pump laser has a high probability of being near the spectral line center. It can be assumed that, on a given spectral line, the lasing occurs on one mode at line center. Large Fresnel number medium pressure flowing lasers, such as cw HF lasers with unstable resonators, generally will fit this assumption quite well.¹⁷

In the cw pump laser used in the early reported work at Hughes, the cross section of the lasing zone in the direction of the resonator is around $(1.2 \times 2.3) \text{ cm}^2$ and the stable resonator is far from confocal (300 cm radius of curvature mirror and flat mirror 70 cm apart). The Fresnel number is around $150 \gg 1$. In this stable cavity, the chemical laser is operated on a number of high order transverse modes and "geometric" modes, thus providing a large number of modes within the spectral linewidth of a lasing transition with fairly uniform spectral and spatial distributions of radiant flux.

It is assumed that the ORTL medium is pressure broadened or homogeneously broadened. The entire population of a specific HF(v,J) state is then available to participate in the resonance absorption or stimulated emission process. There are no so-called hole burning effects.

From real case computations using the linewidth formulae in Appendix B, the pressure broadening width is found, in the Hughes work, to be about equal to the linewidth for Doppler broadening. This calculation for pressure broadening is conservative because the effects of elastic or inelastic long range or grazing collisions have not been included.

With these idealizations in mind, one can formulate the photon interaction as

$$U \frac{dN_u}{dx} = \frac{I(\nu_{ul}; x)}{h\nu_{ul}N_A L} \{1 - \exp[-k(\nu_{ul}; x) L]\}$$

for a differential interaction volume of area $a \times \left[\frac{\sigma_{\text{rad}}(\nu)}{a} \right] (\text{cm}^2)$, and length L (cm), as defined in Fig. 5. The rate of change of N_u (mole/cm), an upper HF(ν, J) state due to the photons, is given by this expression. The flux of pumping laser photons for the transition is $I(x)$ in W/cm^2 at ORTL spectral line center frequency ν_{ul} while h is Planck's constant and N_A is Avogadro's number. The absorption coefficient at line center $k(\nu_{ul})$ (cm^{-1}) is related to the radiative cross section by

$$k(\nu_{ul}) = \sigma_{\text{rad}}(\nu_{ul}) g_1 N_A \left(\frac{N_l}{g_l} - \frac{N_u}{g_u} \right)$$

where g_u and g_l are respectively the rotational statistical weights of upper and lower states of the transition. The derivation has assumed no strong spatial dependences by N_l or N_u in the propagation or L direction and very narrow laser mode widths compared to ORTL medium line widths. An identical interaction expression arises if $I(x)$ versus frequency is nonzero across part of the absorption line, and $k(\nu_{ul}, x)$ is assumed constant within this range. Then $I(x)$ represents the total photon flux across the line. If $I(x)$ lies within the absorption linewidth, the error is not great; the average absorption coefficient within a Gaussian linewidth is $0.79 k(\nu_{ul}, x)$.

Table 6 presents a typical set of inputs for modeling the Hughes ORTL. The double pass coupling of pump laser radiation into the ORTL medium is estimated by multiplying the incoming flux by factor M . The factor is determined by estimating the flux after the first passage through the length L of the medium. Although it is assumed that spatial dependences in that direction are weak, there are noticeable adjustments so M is not quite equal to 2. The density \bar{N}_l averaged in x is determined in an iterative process.

Table 6. ORTL Input Parameters^a

$P_T = 41$ Torr $X_{HF} = 0.03$ $I(x) = 660$ W/cm²

Transition	Flux % Input	Total Influx, W/cm ²	$\nu_{ul}, 10^{14} \text{sec}^{-1}$	A_{ul}, sec^{-1}	$\sigma_g, 10^{-16} \text{cm}^2$	M	$I_0(x), 10^{-3}$
P ₁ (5)	0.07	46.2	1.122	114.0	7.9	1.49	1.94
P ₁ (6)	0.21	138.6	1.108	113.0	8.3	1.66	6.67
P ₁ (7)	0.21	138.6	1.093	113.0	8.75	1.84	7.48
P ₁ (8)	0.05	29.7	1.078	112.0	9.04	1.93	1.71
P ₂ (5)	0.11	72.6	1.073	195.0	14.9	1.56	3.39
P ₂ (6)	0.22	145.2	1.059	193.0	15.6	1.72	7.58
P ₂ (7)	0.10	66.0	1.045	192.0	16.4	1.82	3.69
F ₂ (8)	0.04	25.1	1.030	192.0	17.0	1.94	1.52

$$a_M = 1 + \exp[-\sigma_{\text{rad}}(\nu_{ul})\bar{N}_I L]$$

$$I_0(x) = M I(x)/h\nu_{ul} L N_A, \text{ (mole photons)/(cm}^3\text{sec)}$$

3. MODEL VALIDATION AND SIMULATION OF HUGHES ORTL

The experimental studies on the HF ORTL reported by Bailey et al. of the Hughes Corporation² form the basis for our simulation validation. In their report a careful parametric study was made of a typical ORTL medium. Number densities, static temperatures, and small signal gains were reported. The principal variation was in the partial fraction of HF. The objective of our validation study is to synthesize as many details as possible of the Bailey et al. experimental studies.

A. NUMBER DENSITIES

Comparison of the ORTL model can be made with the Hughes experimental number densities. The pump laser conditions are summarized in Table 6. In terms of Fig. 5, the dimensions of the flux beam are given by $a = 2.3$ cm and $b = 0.38$ cm, while the dimensions of the ORTL flow are $w = 0.3$ cm and $d = 6$ cm. This geometry yields an effective $L = 0.78$. The initial temperature is 300 K and the centerline velocity is 7500 cm/sec (for a parabolic profile with an average velocity of 5000 cm/sec). The model densities of the ORTL medium are determined at the center of the pumping laser beam in the direction of flow (i.e., $x = 0.19$ cm). Individual HF(v, J) populations were summed over J for each level. The corresponding model results are shown in Fig. 6a along with experimental results reported by Bailey et al. The independent variable is the HF initial mole fraction. It is apparent that the agreement is very good. Similar agreement is achieved at $X_{HF} = 0.01$ and for HF(2) at $X_{HF} = 0.03$ in Fig. 6b, for the higher pressure (and higher HF density) ORTL medium condition. It would appear that the most apparent reason for the disagreement is a nominal HF loss (or a smaller than nominal HF flow) in the experiments at 78 Torr. A summation of experimental HF densities for $X_{HF} = 0.03$ yields 4.3×10^{16} particles/cm³. A calculation using nominal pressure data gives 7.5×10^{16} particles/cm³ at 300 K or 400 K under the constant density assumption. The latter temperature is the value computed by the ORTL model during laser pumping. The experimental density of HF is 0.57 of nominal value, which was used in the computer runs. If the experimental data were translated to $X_{HF} = 0.017$, equivalent to 0.57 of nominal X_{HF} , agreement would be greatly improved.

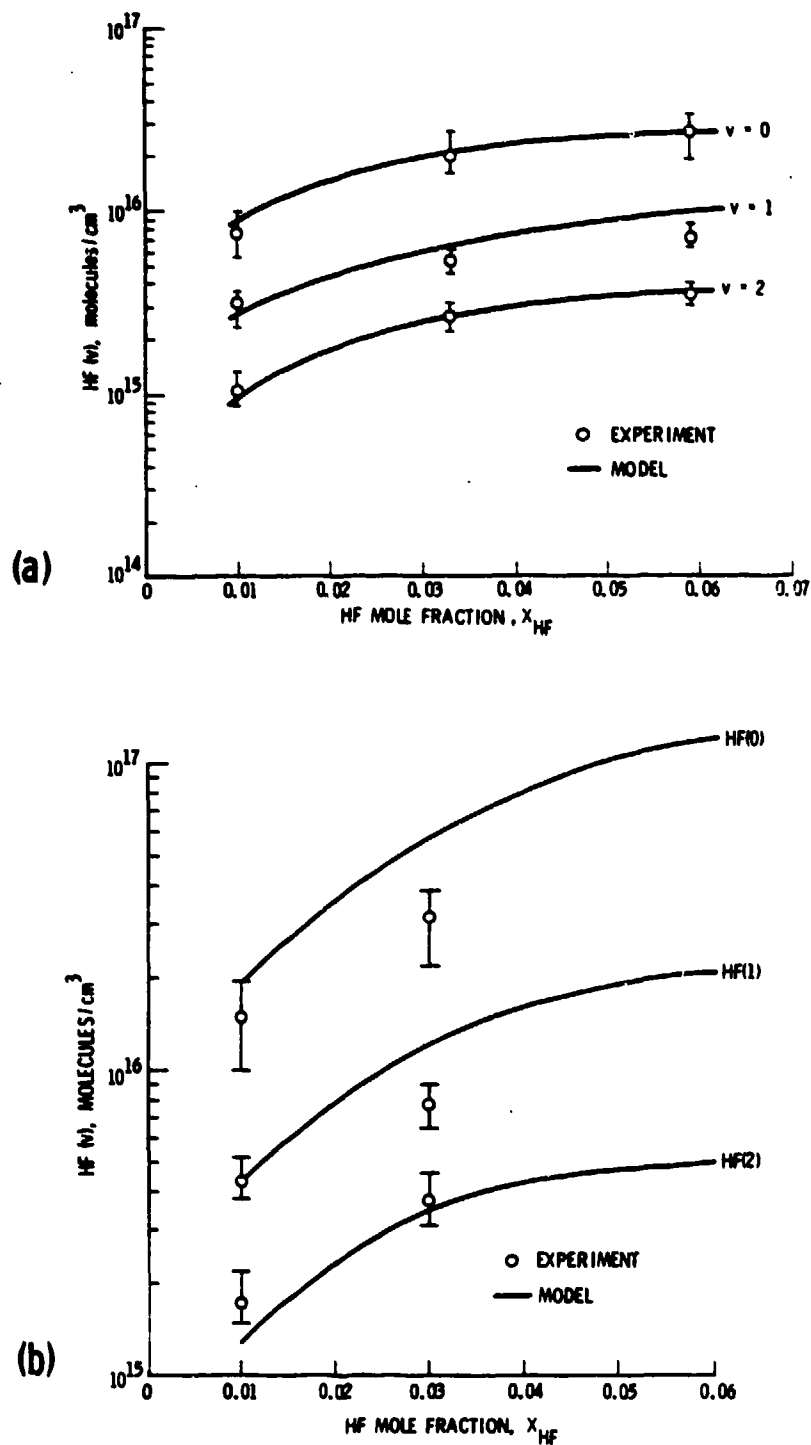


Fig. 6. Comparison of ORTL model and experiments of ORTL medium HF(v) number densities as a function of HF mole fraction. (a) $P=41$ Torr, and (b) $P=78$ Torr. Flux = 660 W/cm^2 , $T=300^\circ\text{K}$, $J_p=4$.

In agreement with experimental results, rotational nonequilibrium effects are not evident at these time scales on the centerline of the pumping beam.

B. STATIC TEMPERATURE

The model results are shown in Fig. 7 for static temperature in the 41 Torr cases. The model static temperature data are likewise extracted from the $x = 0.19$ cm position. The comparison with experimental results is also given. Generally, the model temperatures are from 5 to 10% lower than observed rotational temperatures. Unlike the vibrational number densities, which rise to a nearly uniform condition, the static temperature steadily rises in the flow direction throughout the pumping laser flux field due obviously to the absorption of laser power. The positioning of observation for comparison with model calculations is therefore crucial. It is possible that this is the basis for slight disagreement.

C. SMALL SIGNAL GAINS

Model predictions are in general qualitative agreement with reported observations of zero power gain coefficients. In Figs. 8a and 8b, plots are shown of the gain coefficients g_0 at spectral line center of positive gain HF transitions as a function of flow direction through the pump laser beam. These plots are for the flux of 660 W/cm^2 of the pump laser with the pump line distribution tabulated in Table 6. The initial total pressure is 41 Torr, and the initial static temperature is 300°K with 0.03 HF in He. The largest gain coefficients for our model are in general agreement with the Hughes observations between 0.012 and 0.06 cm^{-1} at the centerline of the pump beam. Since the Hughes data are computed from chemiluminescence number densities on the centerline of the pump beam, the comparable result with our model is 0.01 cm^{-1} on $P_2(8)$ at $x = 0.19 \text{ cm}$ ($t = 36 \text{ } \mu\text{sec}$). The model gain coefficients are seen to rise virtually linearly with distance from a threshold. This behavior suggests that the radiative pump flux levels are too low in these early experiments. On this basis, one projects inefficient recycling of HF molecules and extremely inefficient ORTL lasing. Indeed, the overall efficiency was observed to be around 2%. Alternatively, if the velocity were slowed so a fluid element could spend more time within the beam and reach pumping saturation, a recycling condition can occur, thereby improving greatly the

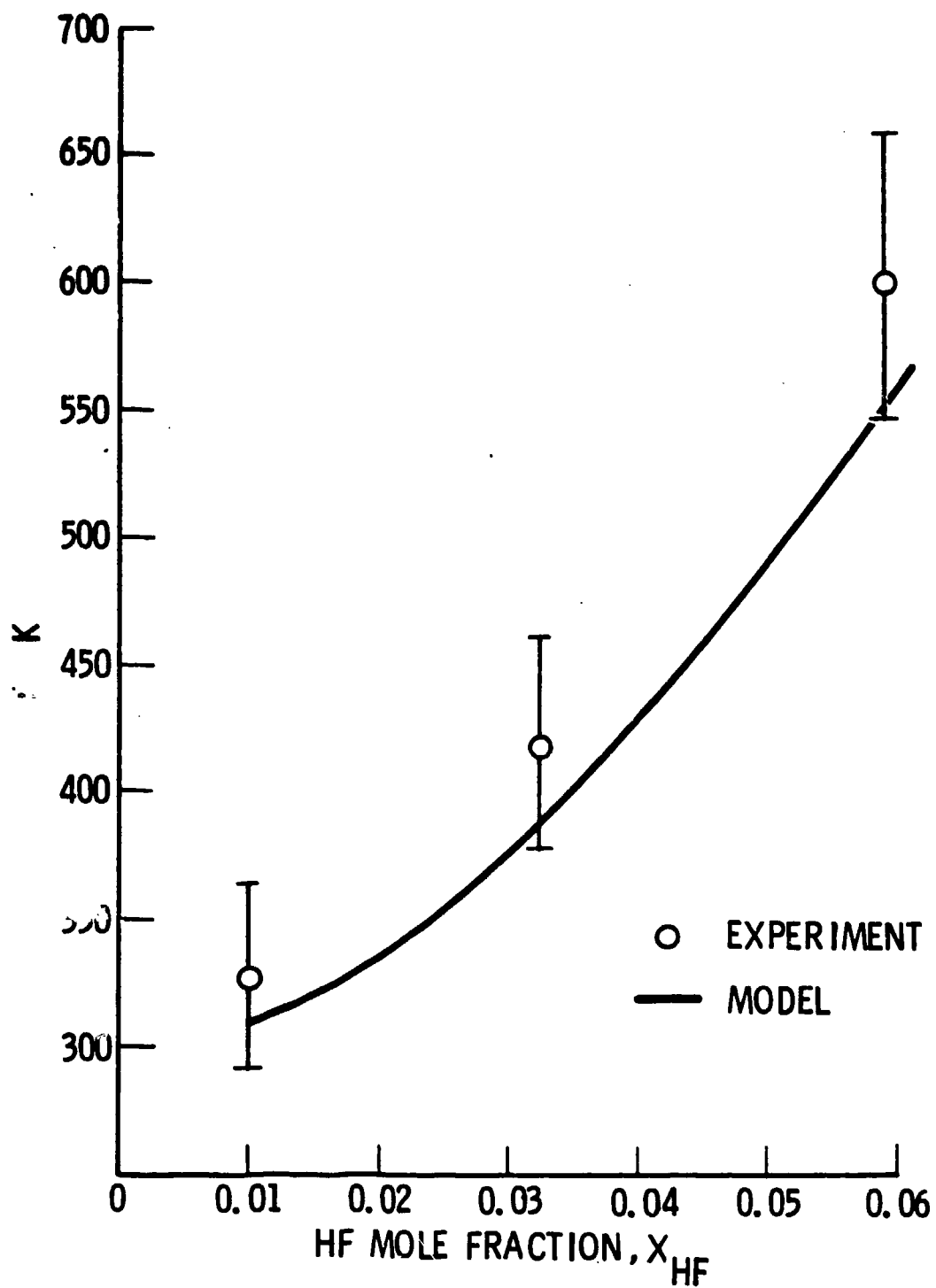


Fig. 7. ORTL medium static temperature as a function of HF mole fraction. Flux=660 W/cm², P=41 Torr, T=300 K, $J_p=5$.

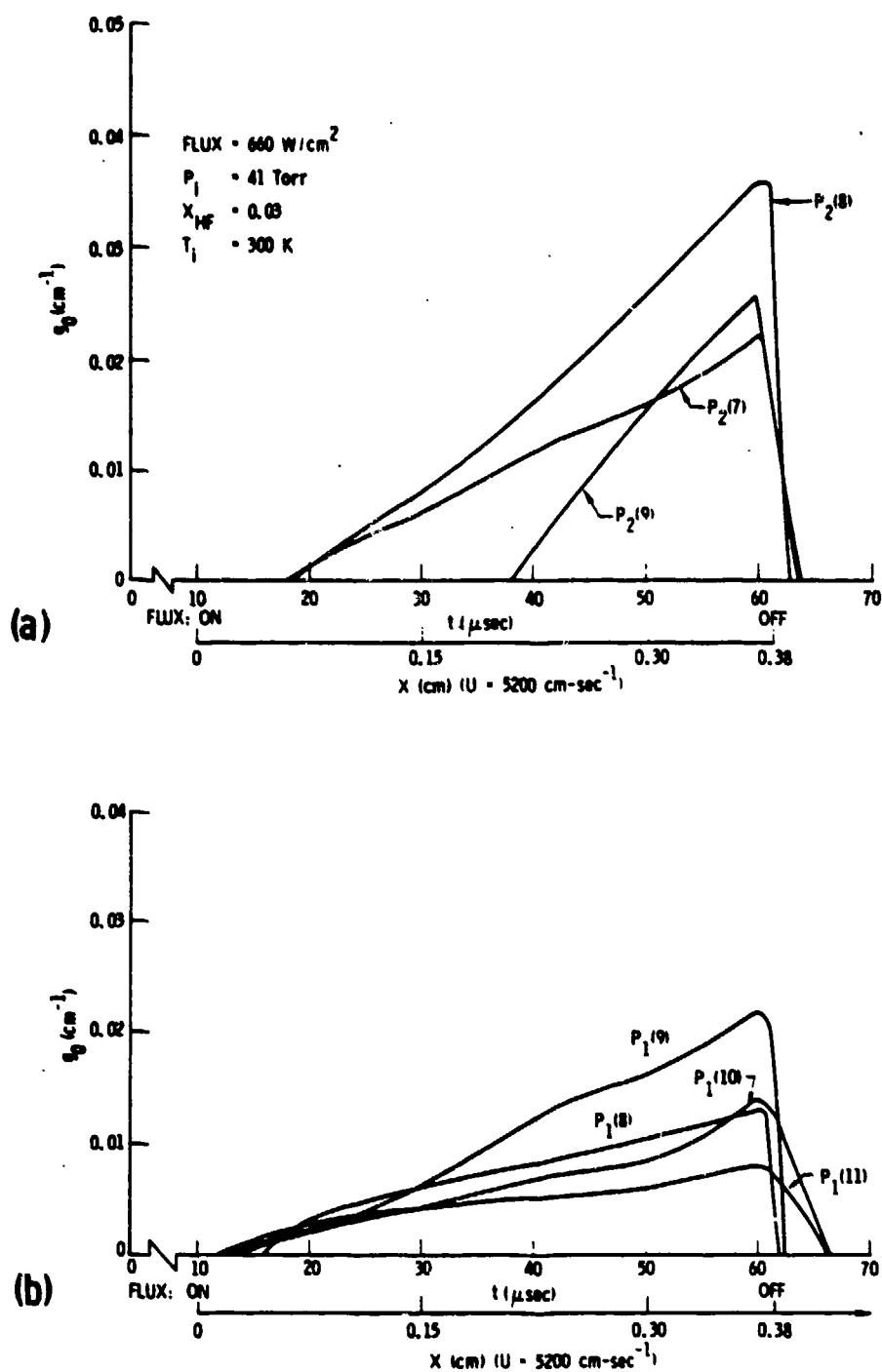


Fig. 8. Small signal gain coefficients as a function of flow distance X or time t . Initial conditions as shown in Table 6. (a) $P_{2+1}(J)$ lines, and (b) $P_{1+0}(J)$ lines.

efficiency of the ORTL. Later Hughes results showed that a factor-of-4 slowing in velocity leads to an order of magnitude improvement in efficiency.

A further comparison of experimental and model results is given in Table 7 where the lasing results are compared with model small signal gain results. The normalization of results is made to one of the better cases, i.e., 440 W/cm² case with P₁(4) and P₂(4) pumping at 78 Torr total pressure and 3% HF. The model small signal gain coefficients for this table are taken at the $x = 0.38$ cm position. The largest gain coefficient at this position is used. This is because some gain plots exhibit the triangular structure in Figure 8 while others do not, depending on conditions. In reality, the axis for the experimental lasing may be at some position equivalent to smaller x .

Table 7. Observed Lasing Compared to Model Gain Coefficient

Case	Pump Lasers (W/cm ²)	Pressure (Torr)	X _{HF}	Normalized Lasing (From Fig. 4 of Ref. 2)	Normalized Model Gain Coefficient
1.	440	78	0.03	1.0	1.0
2.	440	78	0.01	1.0	0.9
3.	440	78	0.06	0.0	0.0
4.	660	78	0.01	0.5	0.2
5.	660	78	0.03	0.8	0.6
6.	660	78	0.06	0.0	0.0
7.	660	41	0.01	<0.05	0.2
8.	660	41	0.03	0.5	0.9
9.	660	41	0.06	0.75	2.2

The agreement is fairly good even on a quantitative basis. Case 7 must describe a case too close to experimental threshold where lasing output is quite sensitive to slight variations. In Case 9 the model gain coefficient, at $P_2(10)$, is somewhat overpredicted. Since most relevant ORTL studies will concentrate on the X_{HF} regime less than 0.03, this deviation is not considered serious for present applications.

The spatial behavior of the gain coefficients in the direction of flow can be summarized using the conditions equivalent to Cases 7, 8, and 9 at 41 Torr, variable X_{HF} at fixed laser pumping flux. As shown in Fig. 9, at $X_{HF} = 0.01$, a steady state in gain is reached rather rapidly after the fluid element enters the beam. However, the steady state small signal gain coefficients are quite low. The $X_{HF} = 0.03$ condition exhibits triangular behavior beginning at the upstream edge of the pump beam, $x = 0$, in Fig. 8. The $X_{HF} = 0.06$ condition shows the same behavior, except the threshold of gain is halfway through the beam, $x = 0.19$ cm, and the growth of gain is steeper to larger final values. The condition is very far from achieving final steady state. Similar model results are produced at 78 Torr. For a given radiative flux level of pumping and for a given density of HF, it is apparent that there is an optimum characteristic time for the gain on a given line to reach empirical steady state. This is not surprising. What is important is that this characteristic time may be unexpectedly long although individual channel processes may have time estimates shorter than 10 μ sec, as noted in the previous section. Obviously, a fluid element should remain in the beam at least as long as this characteristic time, and the effective time for an ORTL "cycle" would be greater than or equal to this characteristic time, which reflects the efficacy of the radiative and collisional pumping processes of the ORTL. The parametric dependent of this characteristic time will be examined later.

D. SENSITIVITY OF ORTL TO COLLISIONAL PROCESSES

The simplest, global assessment of the relative importance of the R-R and V-V processes is by directly removing those particular cross sections in the modeling code and running a particular case. If one chooses the case described in Fig. 8, also labeled No. 8 in Table 7, and removes the R-R cross

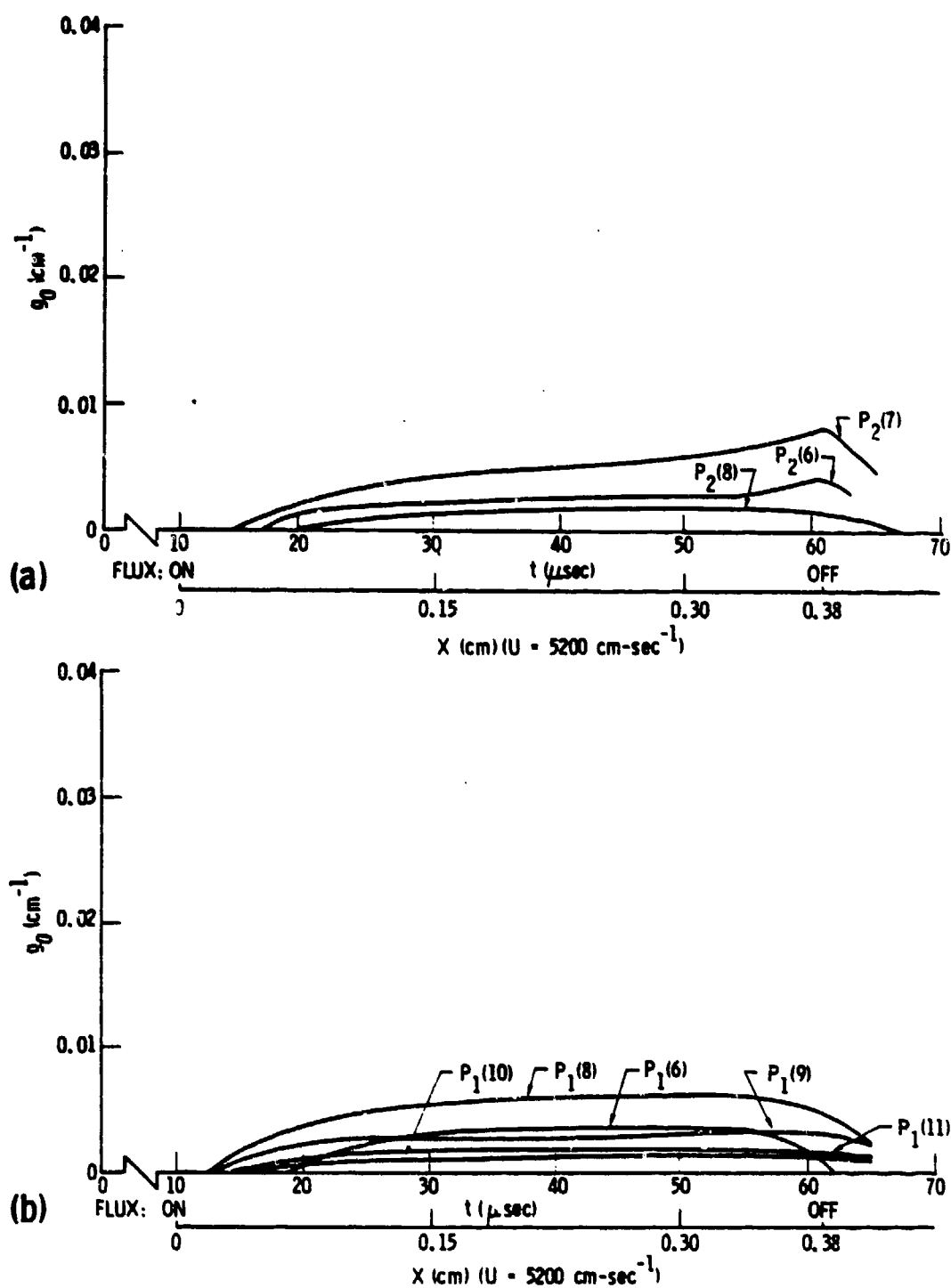


Fig. 9 Small signal gain coefficients as a function of flow distance X or time t . For $X_{HF} = 0.01$. (a) $P_{2+1}(J)$ lines, and (b) $P_{1+0}(J)$ lines.

sections, one produces no positive gain greater than 0.001 cm^{-1} at $x = 0.38 \text{ cm}$ in $P_1(6)$ and $P_1(7)$. This illustrates that the R-R collisional processes are important in $v=1$ or $v=2$ in producing ORTL gain at higher J states than those that are pumped by the laser. This observation is further supported by the modeling results in Fig. 10 for the same ORTL case (660 W/cm^2 , 41 Torr , $X_{\text{HF}} = 0.03$) when the V-V processes are removed. Gain coefficients on the $P_1 \rightarrow 0 (J)$ branch are unaffected (see Fig. 8). In fact, they are larger because the $\text{HF}(v=1)$ states have not been depleted by collisional V-V pumping to $\text{HF}(v=2)$. However, gain coefficients on the $P_2 \rightarrow 1(J)$ branch are greatly affected by the absence of the $1 + 1 \rightarrow 0 + 2$ V + V collisional mechanisms. Since one of the potential benefits of ORTL is the conversion of multiline chemical laser operation to near single-line ORTL lasing at an elevated v level, such as $v=2$, the V-V processes are likewise crucial in producing the relatively large gains on important lines of the $P_2 \rightarrow 1(J)$ branch of HF.

A limited sensitivity study of the R-R and V-V rate sets has also been attempted with an earlier version of the model in which the number of pumping laser lines was five, and the number of kinetic channels available was one-third. This limited us then to an incomplete expression of the V-V processes. The general outcome of these early studies indicated that if the current R-R cross sections were reduced a factor of 3, positive gain would be extinguished on $P_2(8)$. If the R-R cross sections were increased arbitrarily tenfold, not much change occurs to $P_2(8)$ gain. Thus the ORTL provides a lower bound experiment in establishing the sizes of R-R coefficients. The sensitivity of $P_2 \rightarrow 1(J)$ to the V-V processes was observed even in this early work.

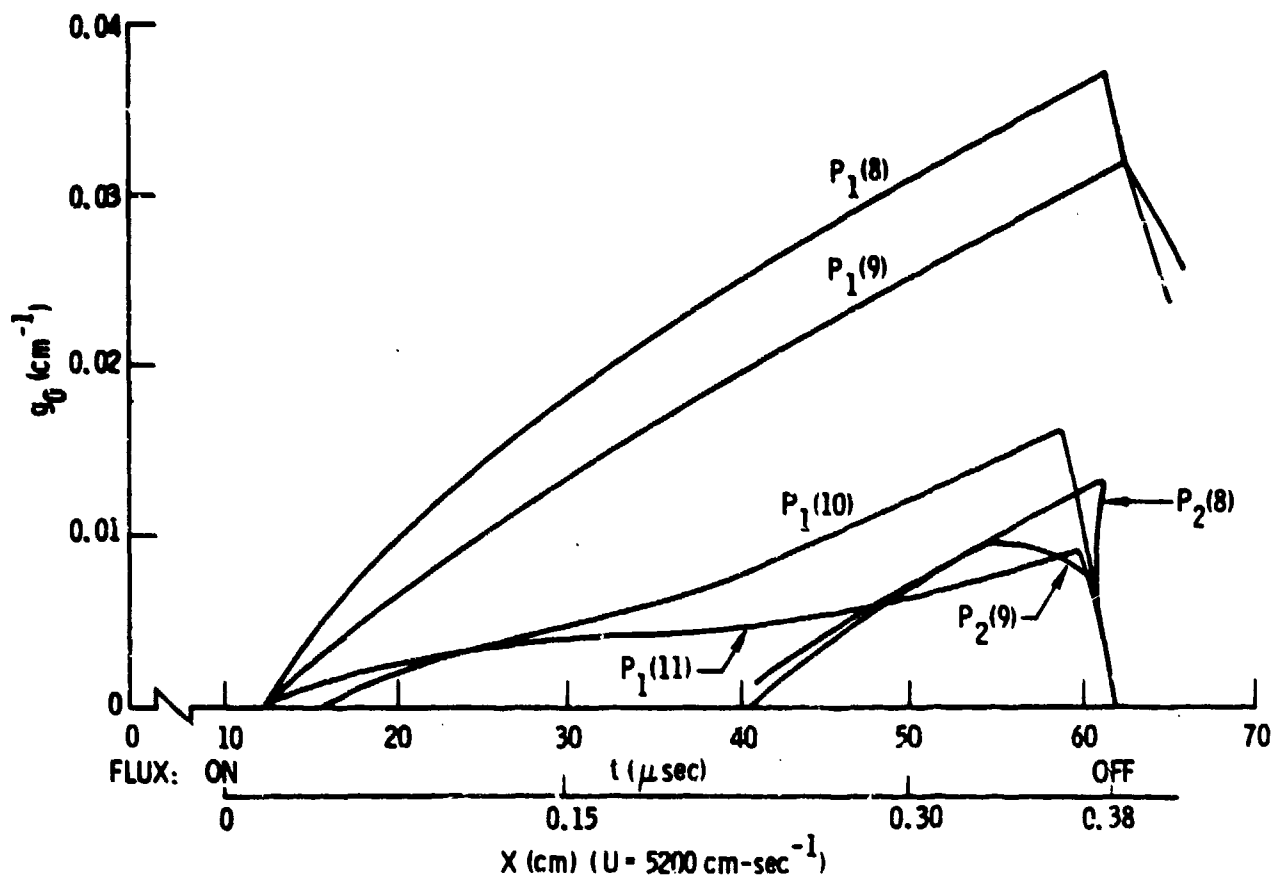


Fig. 10. Case as in Fig. 8, but with V-V rate package removed.

4. ORTL MODEL PARAMETRIC STUDIES

The objective of this section is to explore regimes of ORTL operation in which good overall efficiencies might be expected and short "effective cycle" times might be realized with regard to the sizing of ORTL. Accordingly we will examine the effects of

- a. Flow velocity variation (variation of the time that a fluid element spends in pump beam)
- b. Changes in the J-distributions of pump beam
- c. Pump flux variation
- d. Initial static temperature variation and temperature control.

Since our comparison will deal with small signal gain coefficients, we establish as a baseline case that reported by Hughes as 20 W ORTL output at 78 Torr, $X_{HF} = 0.019$, pumping input at 300 W or 440 W/cm² with a $P_1(4)$ -- $P_1(7)$, $P_2(4)$ -- $P_2(7)$ pattern. The input coupling efficiency was 0.41, the conversion efficiency was 0.18, and overall efficiency was 0.053. For that case our modeling yielded a maximum gain coefficient [on $P_2(7)$ or $P_2(8)$] of 0.05 cm⁻¹ on the downstream edge of the beam. At the centerline of the beam, $x = 0.19$ cm, the gain is around 0.020 cm⁻¹.

If one assumes that ORTL is a homogeneously broadened laser in which the spectral line with dominant gain will lase relatively independently of other branch lines, the maximum extractable power P at optimized coupling is given by¹⁸

$$P = \frac{2W_{SAT}}{T} (\sqrt{G_0} - \sqrt{\delta_0})^2 = \frac{2W_{SAT}}{T} G_0$$

where W_{SAT} is the saturation energy inside the cavity, T is one round trip time within the cavity, G_0 is the round trip zero power gain (obviously proportional to the gain coefficient), and δ_0 is the round trip internal cavity loss. In HF lasers, G_0 is usually much greater than δ_0 . The parameter W_{SAT} depends on pumping and quenching parameters (such as cross sections) which are

quite similar for the high J lasing lines of an HF P-branch. Therefore P is approximately proportional to G_0 at high levels of gain, and we shall utilize this dependence.

A. FLOW VELOCITY

One principal flow adjustment is the velocity of the flow. Basically this variation adjusts the time that any fluid element spends within the pump laser beam. In Fig. 11, the $P_2(J)$ gain coefficients are shown as a function of x for a case in which the velocity is a factor of 4 slower than cases previously discussed, i.e., 1300 cm/sec. The pump flux level is 440 W/cm² with a P(4)--P(7) pattern, and the other flow parameters are an initial pressure of 78 Torr, initial temperature 300 K, and $X_{HF} = 0.03$. A concurrent set of $P_1(J)$ gain coefficients at half the values shown is also generated.

It is quite clear that there is considerable improvement in peak gains around 0.095 cm⁻¹ or a $G_0 \sim 1.2$. This is a four-fold to five-fold improvement on the original Hughes reported results on gain. Using the proportion one can estimate that overall efficiency should improve from 20 to 26% with the significant changes in the conversion efficiency. In fact, this advance has been experimentally reported in unpublished Hughes results, in which overall efficiencies between 25 and 30% were observed. The dominant $P_2(J)$ spectra, according to the model, would shift to higher J states than $P_2(8)$ under these conditions.

The results in Fig. 11 also serve to reinforce the previous remark that, for a given pump flux level and HF density, there is a minimum characteristic time for the fluid element to remain in the beam. In the depicted case, this minimum time appears to be 30 μ sec and the number of possible HF molecular "cycles" might be 5 or 6, out to 150 μ sec.

B. PUMP J-DISTRIBUTION

The pattern of pump HF chemical laser lines is crucial to the potential success of the ORTL concept. Accordingly, a modeling study has been conducted in which the flux input pattern has been varied in J in the following manner. The input flux intensity pattern in Table 6 is maintained; however, the J

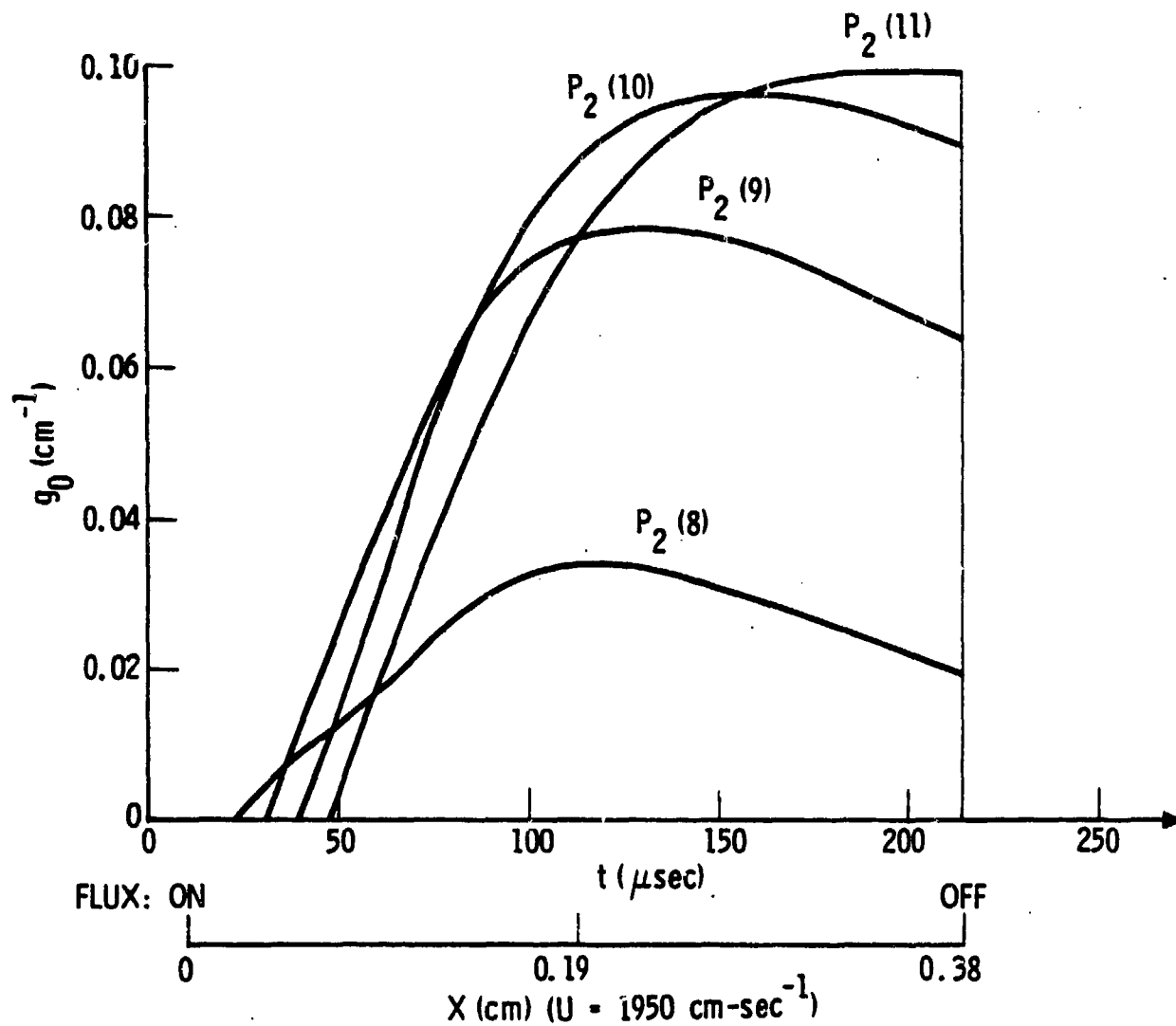


Fig. 11. Small signal gain coefficients as a function of t or X at nearly four-fold slower flow velocity. Only $P_2(J)$ branch lines are presented. Flux=440 W/cm², P =78 Torr, X_{HF} =0.03, T =300 K, and J_p =4 pump flux distribution.

pattern on both the $P_2 + 1$ and $P_1 + 0$ branches will be shifted. The lowest J in the $P(J)$ branch will be designated J_p as an identification of the pattern, i.e., $J = 2$ represents a $P_1(2)$, $P_1(3)$, $P_1(4)$, $P_1(5)$, $P_2(2)$, $P_2(3)$, $P_2(4)$, $P_2(5)$ pattern. For a total flux of 660 W/cm^2 at 41 Torr, 300°K , the results are exhibited in Fig. 12. The maximum achievable gain coefficient is plotted as a function of J_p . It can be seen, unsurprisingly, that an ORTL medium can work very well at low J_p pumping patterns and would probably approach very high overall efficiencies. This is the result of high densities for resonance absorption at the nearly-Boltzmannized lower J HF states and also the result of very fast R-R,T rates at these low J patterns. At higher J , middle J_p around 5 or 6, the peak gain coefficient appears to settle above 0.08 cm^{-1} for $X_{\text{HF}} = 0.03$ and 0.06 . This is equivalent to possible overall efficiencies above 20%, everything else held equal. The peak gain has been driven down mainly by the steady increases in static temperature shown in Fig. 13. These temperatures at the downstream side are large, and therefore with the given positive gain, the inversions (ratios of upper state density to lower state density) are quite high. These great inversions must be partly due to the match of pump spectra with the near-Boltzmann distribution in HF population at the elevated temperatures above 1000°K .

Fig. 14 illustrates that the $P_2(J)$ line of peak gain moves to higher J as J_p , the lowest pump line, increases. This peak gain line always occurs at J greater than J_p . It reflects the fact that the inversions are found at higher J where the lower state densities are initially dropping. In this sense, the peak $P_2(J)$ lasing line in ORTL depends on the pump laser design.

It should be noted, as in Figs. 8 and 11, that significant gain coefficients are generated on lines that are simultaneously pumped by the chemical laser at all patterns of J_p . This behavior would tend to lower the input coupling efficiency as certain strong pump lines are effectively enhanced in passage through the ORTL medium and are not absorbed. Too thick an ORTL medium in the direction of the pump laser beam propagation will obviously convert the ORTL medium to an inefficient amplifier for some lines. At low J_p , where the gain coefficients are large, this problem will have a great influence in lowering the coupling efficiency.

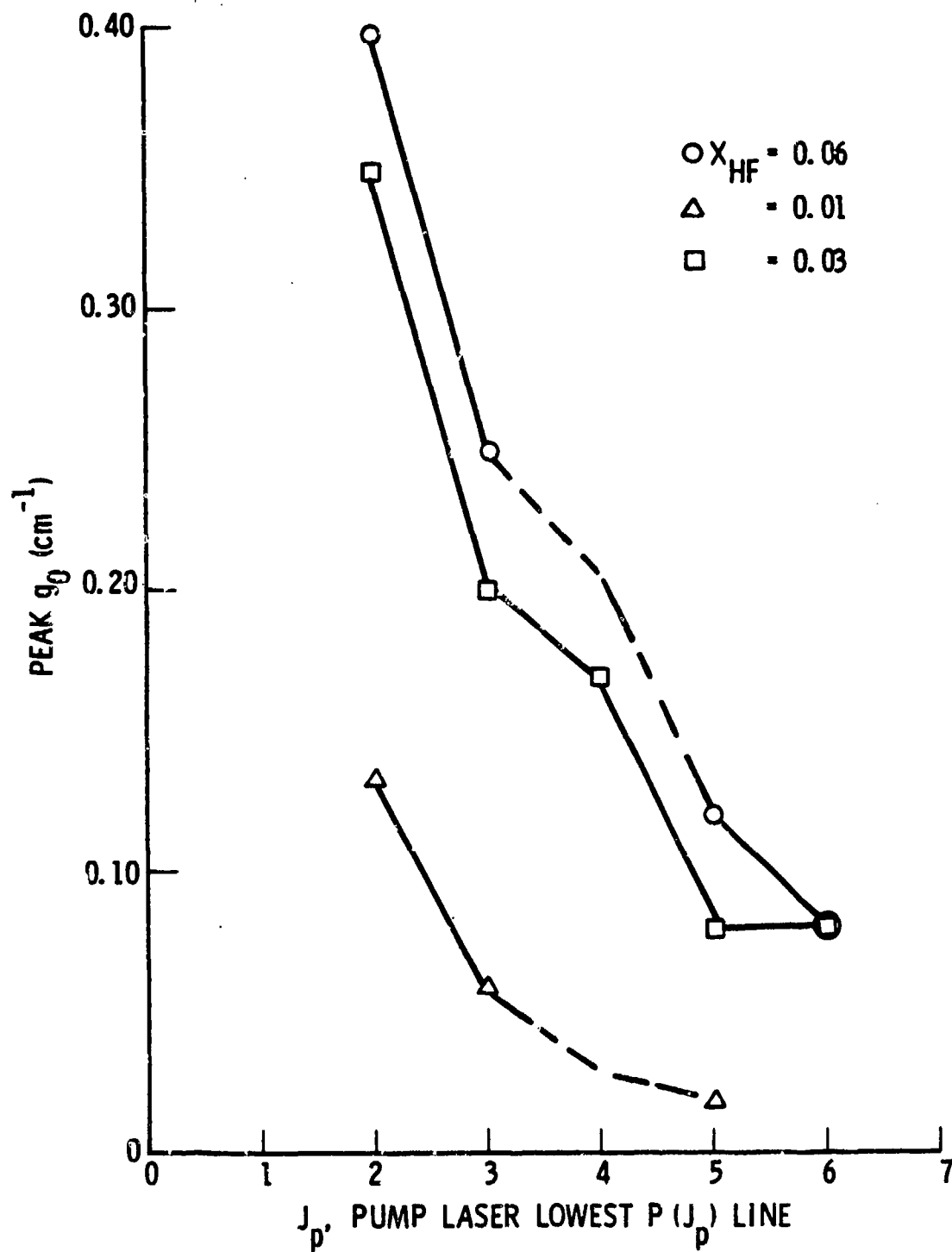


Fig. 12. The dependence of peak gain coefficient on pump flux J distribution. Flux = 660 W/cm^2 , $P = 41 \text{ Torr}$, $T = 300 \text{ K}$.

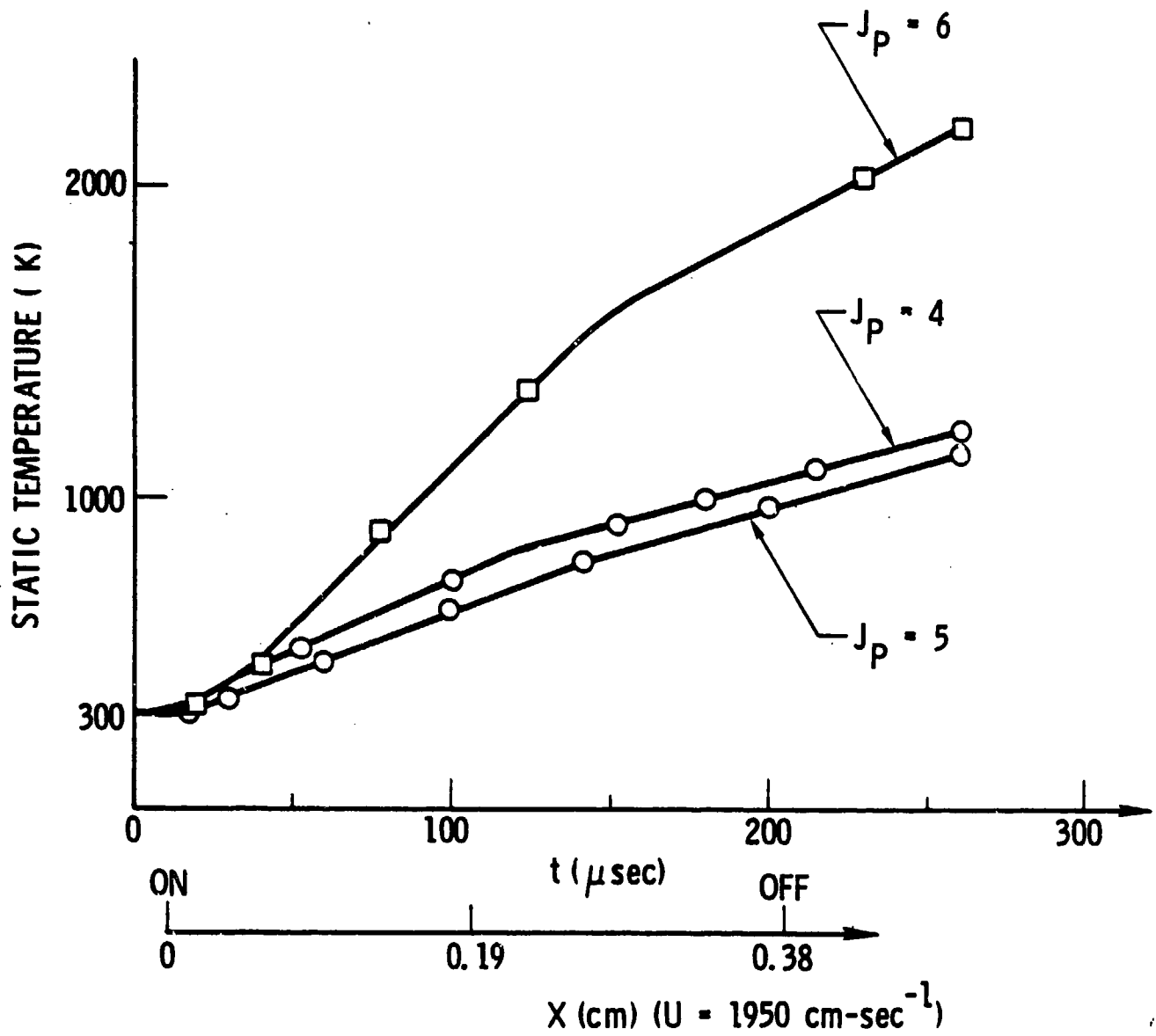


Fig. 13. The effect of gas heating on static temperature in the direction of ORTL gas flow with pump flux J distribution as a variable. Flux=660 W/cm^2 , $P=41$ Torr, $T=300$ K.

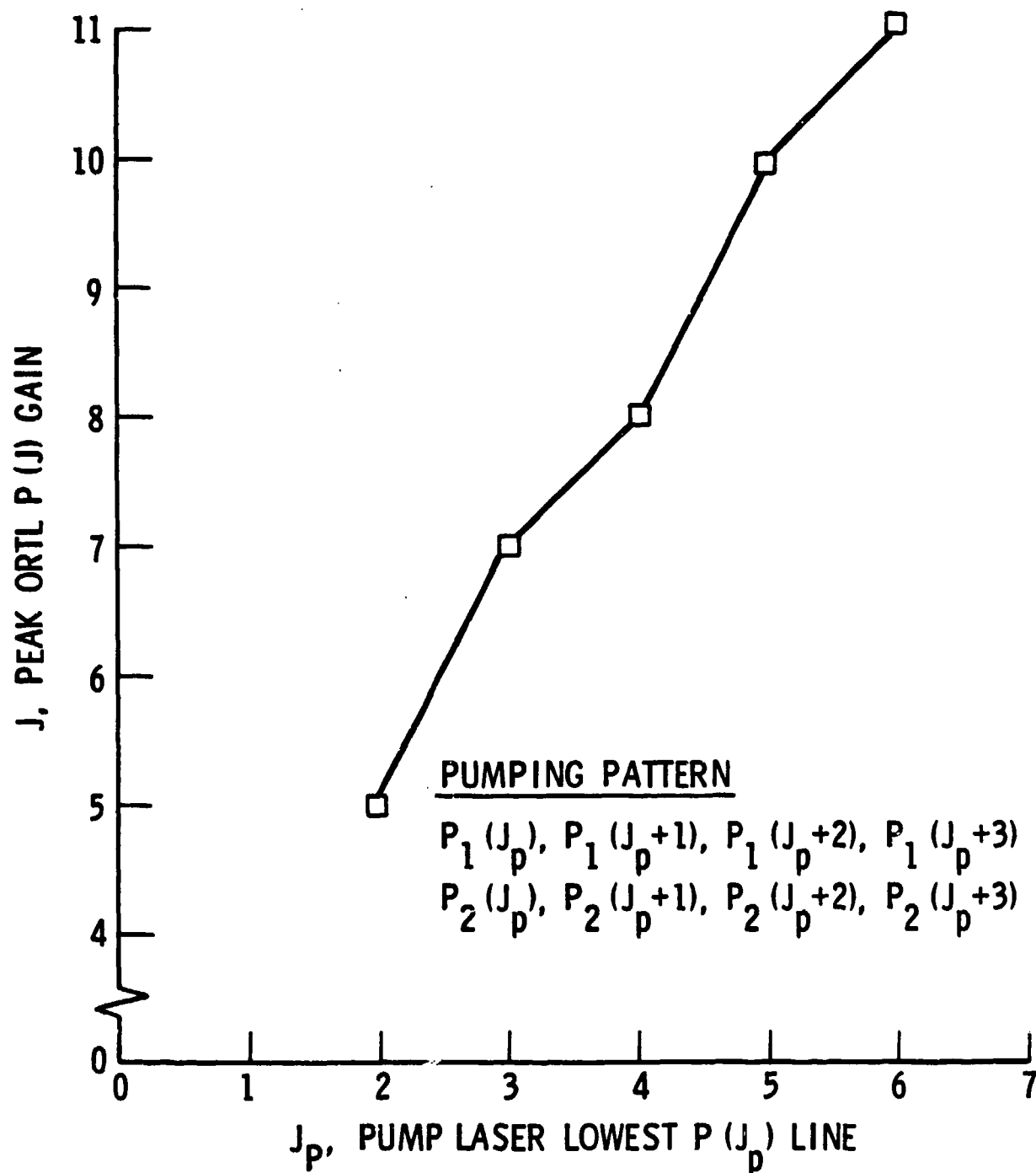


Fig. 14. The shift to higher J in the peak gain $P_{2+1}(J)$ ORTL transition as pump flux J distribution shifts to higher J . Flux = 660 W/cm^{-2} , $P=41 \text{ Torr}$, $T=300 \text{ K}$, $X_{\text{HF}}=0.03$.

The steady temperature rise (Fig. 13) is due to the overall absorption of large amounts of pump radiation. Needless to say, the overall efficiency of ORTL is not unity, and the pump power which is not extractable as ORTL lasing will eventually heat the gas. As the size of the medium grows in larger devices such that the characteristic times for a fluid element within a pump beam become longer, heating mechanisms become more important. On these time scales, this gas heating results from the R-T rates and may be a sensitive indicator for the correct rate scheme here. The gas heating problem is aggravated at intermediate J patterns since the energy gaps in transferring from J to $(J-1)$ on a given vibrational level are increasing proportional to J . From this model study, it seems clear that gas temperature control is an important consideration in ORTL. At the elevated temperatures above 1000 K, it must be noted that the kinetics scheme is no longer completely accurate because literally tens of thousands of V-V channels with energy defects below 1000 cm^{-1} have not been included. Some slight adjustments on V-R collision partners should also have been made. Nevertheless, the model still reflects the general qualitative behavior of the ORTL medium.

C. PUMP FLUX VARIATIONS

As shown in Fig. 11, it is quite clear that the total pump fluxes of the early Hughes studies were too low to be efficient. This limitation was also discussed in Section 2. If the flux is raised to $50,000\text{ W/cm}^2$ for the case in Fig. 11, the peak gain coefficient is attained in $40\text{ }\mu\text{sec}$ rather than $150\text{ }\mu\text{sec}$. This should also improve the effective cycle time on a microscopic basis since radiative pumping times are much faster. In Fig. 15, the effect of flux increases on peak gain coefficient is shown. For an optimum ORTL condition, it appears that the pumping flux should exceed 5000 W/cm^2 or 600 W/cm^2 per pump lasing spectral line. At sufficiently elevated fluxes, there is the additional advantage that the peak gain is attained before gas heating becomes a serious problem in the flow direction. Typically the static temperature does not exceed 1000 K at the peak gain in these cases. For the cases with $J_p = 4$, Fig. 15 shows that an ORTL could operate with 50% overall efficiency.

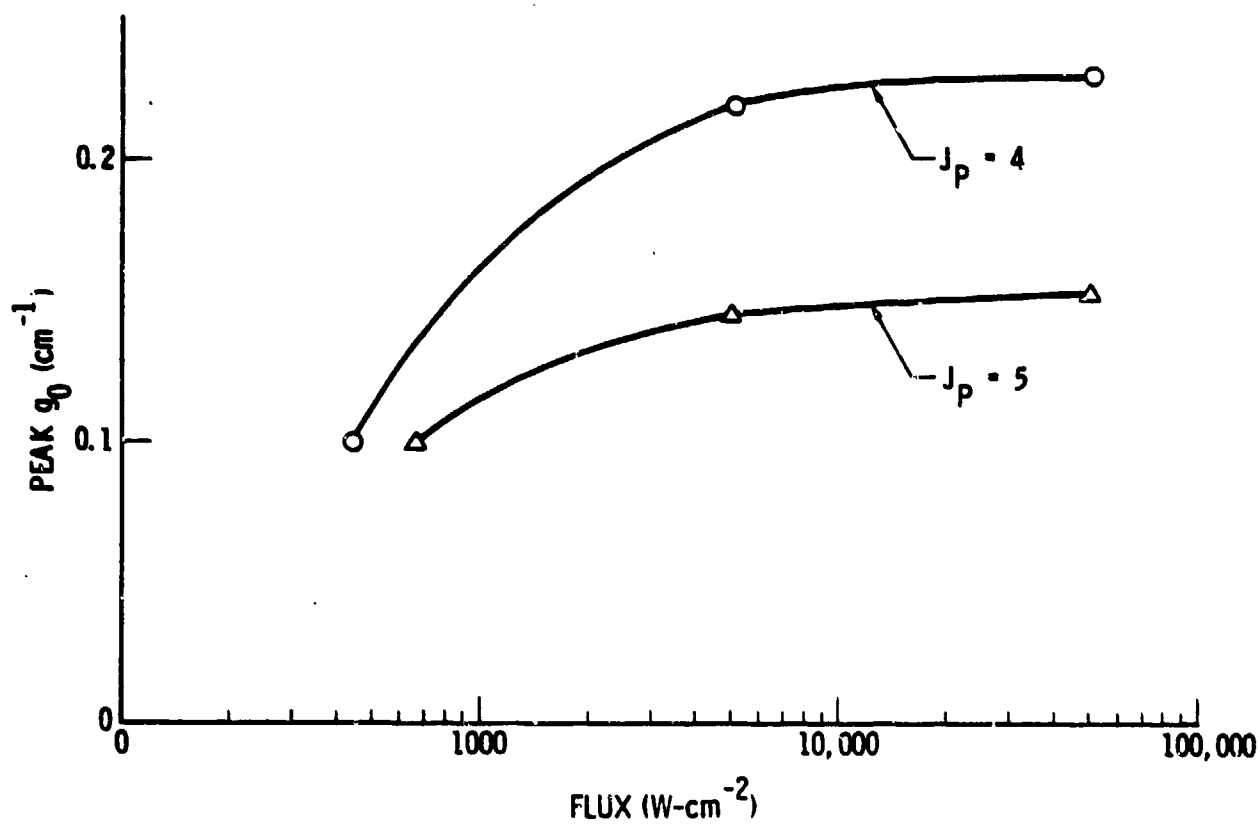


Fig. 15. The dependence of peak gain coefficient on total pumping radiative flux. $P=78$ Torr, $T=300$ K, $X_{\text{HF}}=0.03$.

D. TEMPERATURE

Temperature emerges as an important variable in any cw HF ORTL device. Two aspects of temperature effects have been studied with this ORTL model. The effect of initial temperature of the flow has been examined. Then the possible control of gas heating by the pump laser beam is briefly discussed.

Setting the initial temperature can have two effects in an ORTL. The temperature can be raised such that the initial distribution of $\text{HF}(v=0, J)$ densities better matches the pump laser spectral distribution. The obvious practical limit is reached quickly, however. For $J_p = 6$, an initial ORTL medium temperature around 2000 K would have to be produced for good matching. Even if the practical limit was not a factor, the gain coefficients would generally be lower because of their adverse dependence on temperature. Further, as J_p increases such that the pump laser spectral pattern moves to higher J patterns, one encounters slower R-R, T collisional cross sections, as depicted in Fig. 2.

The second effect of initial temperature is more subtle. In Fig. 16, small signal gain coefficients are plotted as a function of x or t for a case in which the initial temperature is slightly elevated. The case is identical to that shown in Fig. 8 except for the initial temperature. The temperature dependence of the R-R and V-V rate coefficients is such that the coefficients are faster at elevated temperatures. Steady state is apparently reached quite quickly although the peak gain is about half that reported with the initial temperature at 300 K. The temperature rise is under 100 K. The reaching of a peak gain condition in 1 to 2 μsec at such low fluxes is important in establishing an effective "cycle time" for the kinetics, and this characteristic time will determine the ultimate size of ORTL flows relative to pump chemical laser flows. Thus the slight heating of the ORTL medium may be beneficial, at the cost of some of the gain.

Control of gas heating by the pump beam can occur in two ways. If the overall efficiency of the ORTL is unity, there will be no gas heating. Thus power extraction from ORTL lasing is important in moderating the effects of gas heating. The current model examines the worst case, in which no

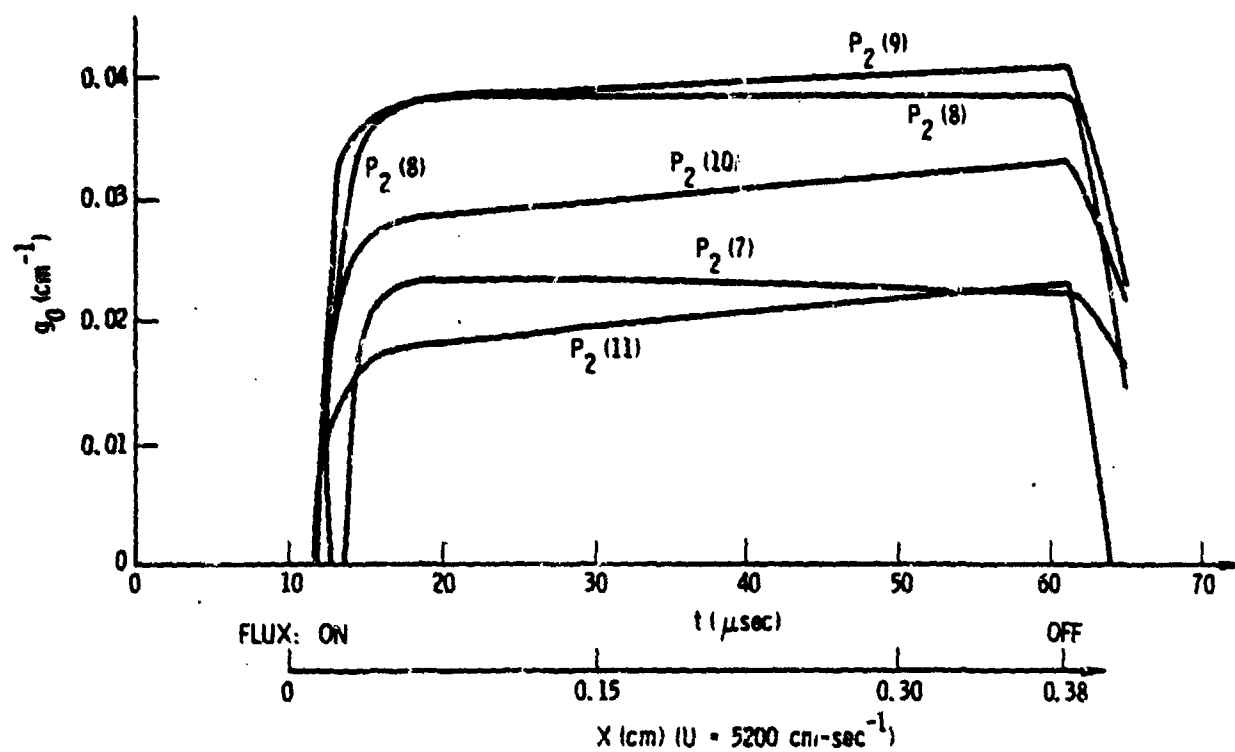


Fig. 16. The effect of elevated initial static temperature, 700 K, on $P_{2+1}(J)$ small signal gain coefficients. The case illustrated is similar to that shown in Fig. 8.

laser power is extracted. A manipulation of the specific heat C_p of the gas can be effected by adding a high C_p species, but poor HF quencher, such as SF_6 in small quantities. For a 78 Torr case, some 15 Torr of SF_6 has been added. The results are presented in Table 8. One can obtain 70% of the peak gain while temperature is nearly halved.

Table 8. Increase in ORTL Medium Heat Capacity

Conditions	Without SF_6	With SF_6
Initial total static pressure (Torr)	78	93
Initial static temperature (K)	300	300
Mole fraction of HF	0.03	0.03
SF_6 pressure (Torr)	0	15
Pumping laser		
flux (W/cm^2)	660	660
J-distribution	$P_1(5)-P_1(8)$ $P_2(5)-P_2(8)$	$P_1(5)-P_1(8)$ $P_2(5)-P_2(8)$
Final static temperature (at exiting pump beam) (K)	1501	815
Peak gain (cm^{-1})	0.098	0.070
Peak gain line	$P_2(11)$	$P_2(10)$

E. BEST REGIME

In evaluation of the ORTL medium as a gain generator, this modeling study has established that the most attractive regime for a cw HF ORTL might be total pump fluxes in excess of $5000 W/cm^2$, pump spectral pattern with $J_p < 4$, total pressures up to 78 Torr, X_{HF} between 0.01 and 0.03 (for a double pass

coupling mirror system), slightly elevated initial temperatures, high heat capacities in the flow, and fluid element times in the pump beam no longer than 200 μsac . An attractive regime is defined as that with a peak gain exceeding 0.2 cm^{-1} , equivalent to an overall efficiency of 0.5.

5. CONCLUSION

A model has been developed to study the gas flow of an optically resonantly pumped transfer laser as an efficient gain generator. A criterion of 0.20 cm^{-1} for the peak gain coefficient has been used as equivalent to an overall efficiency of 50 percent. The equivalence was established in this model of small signal gain by simulating reported Hughes experiments. This evaluation has been conducted to determine if the ORTL device might efficiently convert the beam of a high power cw HF chemical laser into a laser beam of the highest quality.

A regime has been found by the model in which the 0.20 cm^{-1} criterion is met and exceeded. This regime requires the pump laser to produce:

- a. Greater than 5000 W/cm^2 flux (1000 W/cm^2 in one spectral line)
- b. A pumping pattern with $J_p < 4$ where the lasing lines are

$P_1(J_p=4)$, $P_1(5)$, $P_1(6)$, $P_1(7)$ and

$P_2(J_p=4)$, $P_2(5)$, $P_2(6)$, $P_2(7)$

and over 80% of the power is in the P(5) and P(6) lines of both branches.

The ORTL medium, He and HF, should operate at

- a. Total pressures up to 80 Torr
- b. Elevated initial temperatures up to 600 K for proper flow sizes
- c. HF mole fractions between 0.01 and 0.03 for a double pass coupling mirror system for the pump laser.

For a multiple-pass coupling mirror system the mole fraction would be proportionally reduced (10 passes, one-fifth the mole fraction listed). The optical depth for the pump laser beams total passage through the medium should be unity.

To achieve an attractive ORTL sizing relative to cw chemical laser flows, the ORTL medium velocity should be around 10^4 cm/sec^{-1} . Any fluid element should be in the pump beam for a period exceeding 100 μsec . In this way, the typical HF molecules can be "reused" cyclicly many times. The minimum cycle

time is, of course, determined by the flux level, concentrations, and the effect of elevated static temperature on rate coefficients. In this identified regime, the ORTL flow at a higher velocity could be a fraction of the size of the cw chemical laser nozzle area, as suggested in Table 1. It should be noted that this discussion does not include systems considerations such as reservoir tanks and exhaust systems.

The principal problems and limitations of the ORTL medium have also been observed with this simple model. The favorable spectral line distribution required for high efficiency tends toward lower J P-branch lines at or below P(5) and P(6). This distribution is not typical of most efficient cw HF lasers, which tend toward higher J lines.

Elevated initial temperature operation appears to be not important in achieving 0.2 cm^{-1} peak gain operation. However, this condition is important in sizing the ORTL. It is an additional operational complication.

The ORTL medium is possibly limited in two of three dimensions by the following considerations. In the direction of propagation of the pump laser, the model has shown that in a multiple line pumping pattern in rotational non-equilibrium, gain can be generated on transitions on which pumping laser lines exist. For too large a dimension (or optical depth), significant amplification will occur. This effectively lowers the input coupling efficiency (and therefore the overall efficiency) and directs power away from improvement in this beam quality. Therefore the shape of the ORTL medium has constraints important to an ORTL resonator designer.

Significant gas heating by pump laser radiation is generated by the small signal gain model at longer time scales in the flow direction. Practically, this effect could limit the extent of the ORTL medium in the flow direction (within the pump beam) to characteristic times below 300 μsec . ORTL lasing would moderate this effect. Additives such as SF_6 augmenting the specific heat of the flow are also helpful in controlling gas heating.

The ORTL concept for improving beam quality could continue to merit serious consideration if the pump laser line distributions ever reach the appropriate medium-to-low J P-branch positions. It is also evident that a

proper evaluation of an actual device will require experiments at the proper scale and size of pumping and ORTL devices. From our flux variation study, it is apparent that a greater than 5000 W/cm^2 pumping laser with an adequate pump beam cross section (i.e., $10\text{--}20 \text{ cm}^2$) is needed to evaluate simultaneously the optimum overall efficiency and true ORTL size relative to the pump laser. The pump device should have a $J_p < 4$ pattern; otherwise the benefits of such an experiment may be limited. Current experiments at smaller scales are limited in value in that they will have difficulty exhibiting satisfactory overall efficiencies or sizes.

Our current model of an ORTL device can be further improved. Further definitive parametric studies should be made. The major model improvement would be the conversion of the current code to a lasing model, at least at the conventional level obtained by using Fabry-Perot mirrors. Then the defined efficiencies of an actual ORTL can directly be estimated. Since parts of the ORTL medium experience large elevated temperatures, a reexamination of $R \rightarrow T$ mechanisms and an expansion of the V-V manifold would seem useful. Modeling of the pump laser coupling can be improved by converting factor M into a density-dependent variable in the flow direction such that pump lines can experience gain as well as absorption. In the current work, $M \sim 2$ because the medium is thin, and any errors have not been large.

Finally, we note that an ORTL device seems an excellent, relevant, empirical test for $EF(v,J) + M$ kinetics and laser modeling of cw HF lasers because of its basic simplicity.

REFERENCES

1. J. H. S. Wang, J. Finzi, and F. N. Mastrup, Appl. Phys. Lett. 31, 35-37 (1977).
2. P. K. Baily, J. Finzi, G. W. Holleman, K. K. Hui, and J. H. S. Wang, High Energy Optical Resonance Transfer Study, Hughes Aircraft Corporation Technical Report FR-79-73-538, Culver City, Calif. (Jan. 1979).
3. K. K. Hui, P. K. Baily, J. Finzi, J. H. S. Wang, and F. N. Mastrup, Appl. Opt. 19, 842-832 (1980).
4. J. Finzi, J. H. S. Wang, K. K. Hui, P. K. Baily, G. W. Holleman, and F. N. Mastrup, IEEE J. Quantum Electron QE-16, 912-914 (1980).
5. J. H. S. Wang, J. Finzi, P. K. Baily, G. W. Holleman, K. K. Hui, and F. N. Mastrup, Appl. Phys. Lett. 36 24-25 (1980).
6. G. W. Holleman and H. Injeyan, Multiwavelength 2-5 Micrometer Laser, Hughes Aircraft Corporation Technical Report FR 80-72-653 (June 1980).
7. R. L. Wilkins and M. A. Kwok, J. Chem. Phys. 73, 3198-3204 (1980).
8. R. L. Wilkins and M. A. Kwok, J. Chem. Phys. 70, 1705-1710 (1979).
9. R. L. Wilkins, J. Chem. Phys. 67, 5838 (1977).
10. R. L. Wilkins, to be published.
11. J. J. Hinchey and R. H. Hobbs, J. Chem. Phys. 65, 2732-2739 (1976).
12. J. J. Hinchey and R. H. Hobbs, J. Appl. Phys. 50, 628-636 (1979).
13. R. L. Wilkins and M. A. Kwok, to be published.
14. R. M. Osgood, Jr., P. B. Sackett, and A. Javan, J. Chem. Phys. 60, 1464-1480 (1974).
15. M. J. Bina and C. R. Jonas, Appl. Phys. Lett. 22, 44-6 (1973).
16. E. B. Turner, G. Emanuel, and R. L. Wilkins, The NEST Chemistry Computer Program, TR-0059(6240-40)-1, The Aerospace Corporation, El Segundo, Calif. (30 June 1970).
17. H. Mirels, AIAA J 17, 478-489 (1979).
18. A. E. Siegman, An Introduction to Lasers and Masers, McGraw Hill Co., New York, (1971), p. 433.

19. M. A. Kwok and R. L. Wilkins, J. Chem. Phys. 63, 2453 (1975).
20. M. A. Kwok and N. Cohen, personal communication.
21. P. R. Poole and J. W. M. Smith, J. Chem. Soc., Faraday Transactions II, 73, 1434 (1977).
22. D. J. Douglas and C. Bradley Moore, Chem. Phys. Lett. 57, 435 (1978).
23. J. Bott, J. Chem. Phys. 57, 961 (1972).
24. J. R. Airey and I. W. M. Smith, J. Chem. Phys. 57, 1669 (1973).
25. G. M. Jursich and F. F. Crim, J. Chem. Phys. 74, 4455 (1981).
26. J. K. Lampert, G. M. Jursich, and F. F. Crim, Chem. Phys. Lett. 71, 258 (1980).
27. G. D. Billing and L. L. Poulsen, J. Chem. Phys. 68, 5120 (1978).
28. H. K. Shin and V. H. Kim, J. Chem. Phys. 64, 3634 (1976).
29. C. Clendening, J. I. Steinfeld, and L. E. Wilson, Information Theory Analysis of Deactivation Rates in Chemical Lasers, AFWL-TR-76-144 (Oct. 1976).

APPENDIX A

KINETICS EQUATION LISTING (Photo Reduced)

	Rate Equation	k_f cm ³ /(mole sec)	A	n	E cal/mole
1	HF(200), + M1 = HF(201), + M1	KF =	.418E19	- .848	- 2565

$$k_f = A T^n \exp (E/RT)$$

7449. 848. 15E+18. KF=
3345. 848. 11E+18. KF=
4345. 848. 16E+18. KF=
5666. 848. 18E+18. KF=
7093. 848. 18E+18. KF=
3453. 848. 19E+18. KF=
4560. 848. 18E+18. KF=
5730. 848. 18E+18. KF=
6569. 848. 18E+18. KF=
7772. 848. 18E+18. KF=
6339. 848. 18E+18. KF=
9229. 848. 18E+18. KF=
3665. 848. 18E+18. KF=
4992. 848. 18E+18. KF=
5469. 848. 18E+18. KF=
1388. 848. 18E+18. KF=
6108. 848. 18E+18. KF=
3227. 848. 18E+18. KF=
10471. 848. 18E+18. KF=
33971. 848. 18E+18. KF=
7018. 848. 18E+18. KF=
9725. 848. 18E+18. KF=
10540. 848. 18E+18. KF=
5992. 848. 18E+18. KF=
7396. 848. 18E+18. KF=
9116. 848. 18E+18. KF=
11020. 848. 18E+18. KF=
4071. 848. 18E+18. KF=
5786. 848. 18E+18. KF=
5599. 848. 18E+18. KF=
1438. 848. 18E+18. KF=
12565. 848. 18E+18. KF=
27330. 848. 18E+18. KF=
3580. 848. 18E+18. KF=
4143. 848. 18E+18. KF=
2017. 848. 18E+18. KF=
3493. 848. 18E+18. KF=
4030. 848. 18E+18. KF=
2791. 848. 18E+18. KF=
3241. 848. 18E+18. KF=
3847. 848. 18E+18. KF=
4526. 848. 18E+18. KF=
5192. 848. 18E+18. KF=
5861. 848. 18E+18. KF=
6530. 848. 18E+18. KF=
7200. 848. 18E+18. KF=
7869. 848. 18E+18. KF=
8538. 848. 18E+18. KF=
9207. 848. 18E+18. KF=
9876. 848. 18E+18. KF=
10545. 848. 18E+18. KF=
11214. 848. 18E+18. KF=
11883. 848. 18E+18. KF=
12552. 848. 18E+18. KF=
13221. 848. 18E+18. KF=
13890. 848. 18E+18. KF=
14559. 848. 18E+18. KF=
15228. 848. 18E+18. KF=
15897. 848. 18E+18. KF=
16566. 848. 18E+18. KF=
17235. 848. 18E+18. KF=
17904. 848. 18E+18. KF=
18573. 848. 18E+18. KF=
19242. 848. 18E+18. KF=
19911. 848. 18E+18. KF=
20580. 848. 18E+18. KF=
21249. 848. 18E+18. KF=
21918. 848. 18E+18. KF=
22587. 848. 18E+18. KF=
23256. 848. 18E+18. KF=
23925. 848. 18E+18. KF=
24594. 848. 18E+18. KF=
25263. 848. 18E+18. KF=
25932. 848. 18E+18. KF=
26601. 848. 18E+18. KF=
27270. 848. 18E+18. KF=
27939. 848. 18E+18. KF=
28608. 848. 18E+18. KF=
29277. 848. 18E+18. KF=
29946. 848. 18E+18. KF=
30615. 848. 18E+18. KF=
31284. 848. 18E+18. KF=
31953. 848. 18E+18. KF=
32622. 848. 18E+18. KF=
33291. 848. 18E+18. KF=
33960. 848. 18E+18. KF=
34629. 848. 18E+18. KF=
35298. 848. 18E+18. KF=
35967. 848. 18E+18. KF=
36636. 848. 18E+18. KF=
37305. 848. 18E+18. KF=
37974. 848. 18E+18. KF=
38643. 848. 18E+18. KF=
39312. 848. 18E+18. KF=
39981. 848. 18E+18. KF=
40650. 848. 18E+18. KF=
41319. 848. 18E+18. KF=
41988. 848. 18E+18. KF=
42657. 848. 18E+18. KF=
43326. 848. 18E+18. KF=
43995. 848. 18E+18. KF=
44664. 848. 18E+18. KF=
45333. 848. 18E+18. KF=
46002. 848. 18E+18. KF=
46671. 848. 18E+18. KF=
47340. 848. 18E+18. KF=
48009. 848. 18E+18. KF=
48678. 848. 18E+18. KF=
49347. 848. 18E+18. KF=
50016. 848. 18E+18. KF=
50685. 848. 18E+18. KF=
51354. 848. 18E+18. KF=
52023. 848. 18E+18. KF=
52692. 848. 18E+18. KF=
53361. 848. 18E+18. KF=
54030. 848. 18E+18. KF=
54699. 848. 18E+18. KF=
55368. 848. 18E+18. KF=
56037. 848. 18E+18. KF=
56706. 848. 18E+18. KF=
57375. 848. 18E+18. KF=
58044. 848. 18E+18. KF=
58713. 848. 18E+18. KF=
59382. 848. 18E+18. KF=
60051. 848. 18E+18. KF=
60720. 848. 18E+18. KF=
61389. 848. 18E+18. KF=
62058. 848. 18E+18. KF=
62727. 848. 18E+18. KF=
63396. 848. 18E+18. KF=
64065. 848. 18E+18. KF=
64734. 848. 18E+18. KF=
65403. 848. 18E+18. KF=
66072. 848. 18E+18. KF=
66741. 848. 18E+18. KF=
67410. 848. 18E+18. KF=
68079. 848. 18E+18. KF=
68748. 848. 18E+18. KF=
69417. 848. 18E+18. KF=
70086. 848. 18E+18. KF=
70755. 848. 18E+18. KF=
71424. 848. 18E+18. KF=
72093. 848. 18E+18. KF=
72762. 848. 18E+18. KF=
73431. 848. 18E+18. KF=
74100. 848. 18E+18. KF=
74769. 848. 18E+18. KF=
75438. 848. 18E+18. KF=
76107. 848. 18E+18. KF=
76776. 848. 18E+18. KF=
77445. 848. 18E+18. KF=
78114. 848. 18E+18. KF=
78783. 848. 18E+18. KF=
79452. 848. 18E+18. KF=
80121. 848. 18E+18. KF=
80790. 848. 18E+18. KF=
81459. 848. 18E+18. KF=
82128. 848. 18E+18. KF=
82797. 848. 18E+18. KF=
83466. 848. 18E+18. KF=
84135. 848. 18E+18. KF=
84804. 848. 18E+18. KF=
85473. 848. 18E+18. KF=
86142. 848. 18E+18. KF=
86811. 848. 18E+18. KF=
87480. 848. 18E+18. KF=
88149. 848. 18E+18. KF=
88818. 848. 18E+18. KF=
89487. 848. 18E+18. KF=
90156. 848. 18E+18. KF=
90825. 848. 18E+18. KF=
91494. 848. 18E+18. KF=
92163. 848. 18E+18. KF=
92832. 848. 18E+18. KF=
93501. 848. 18E+18. KF=
94170. 848. 18E+18. KF=
94839. 848. 18E+18. KF=
95508. 848. 18E+18. KF=
96177. 848. 18E+18. KF=
96846. 848. 18E+18. KF=
97515. 848. 18E+18. KF=
98184. 848. 18E+18. KF=
98853. 848. 18E+18. KF=
99522. 848. 18E+18. KF=
100191. 848. 18E+18. KF=
100860. 848. 18E+18. KF=
101529. 848. 18E+18. KF=
102198. 848. 18E+18. KF=
102867. 848. 18E+18. KF=
103536. 848. 18E+18. KF=
104205. 848. 18E+18. KF=
104874. 848. 18E+18. KF=
105543. 848. 18E+18. KF=
106212. 848. 18E+18. KF=
106881. 848. 18E+18. KF=
107550. 848. 18E+18. KF=
108219. 848. 18E+18. KF=
108888. 848. 18E+18. KF=
109557. 848. 18E+18. KF=
110226. 848. 18E+18. KF=
110895. 848. 18E+18. KF=
111564. 848. 18E+18. KF=
112233. 848. 18E+18. KF=
112902. 848. 18E+18. KF=
113571. 848. 18E+18. KF=
114240. 848. 18E+18. KF=
114909. 848. 18E+18. KF=
115578. 848. 18E+18. KF=
116247. 848. 18E+18. KF=
116916. 848. 18E+18. KF=
117585. 848. 18E+18. KF=
118254. 848. 18E+18. KF=
118923. 848. 18E+18. KF=
119592. 848. 18E+18. KF=
120261. 848. 18E+18. KF=
120930. 848. 18E+18. KF=
121599. 848. 18E+18. KF=
122268. 848. 18E+18. KF=
122937. 848. 18E+18. KF=
123606. 848. 18E+18. KF=
124275. 848. 18E+18. KF=
124944. 848. 18E+18. KF=
125613. 848. 18E+18. KF=
126282. 848. 18E+18. KF=
126951. 848. 18E+18. KF=
127620. 848. 18E+18. KF=
128289. 848. 18E+18. KF=
128958. 848. 18E+18. KF=
129627. 848. 18E+18. KF=
130296. 848. 18E+18. KF=
130965. 848. 18E+18. KF=
131634. 848. 18E+18. KF=
132303. 848. 18E+18. KF=
132972. 848. 18E+18. KF=
133641. 848. 18E+18. KF=
134310. 848. 18E+18. KF=
134979. 848. 18E+18. KF=
135648. 848. 18E+18. KF=
136317. 848. 18E+18. KF=
136986. 848. 18E+18. KF=
137655. 848. 18E+18. KF=
138324. 848. 18E+18. KF=
138993. 848. 18E+18. KF=
139662. 848. 18E+18. KF=
140331. 848. 18E+18. KF=
141000. 848. 18E+18. KF=
141669. 848. 18E+18. KF=
142338. 848. 18E+18. KF=
143007. 848. 18E+18. KF=
143676. 848. 18E+18. KF=
144345. 848. 18E+18. KF=
145014. 848. 18E+18. KF=
145683. 848. 18E+18. KF=
146352. 848. 18E+18. KF=
147021. 848. 18E+18. KF=
147690. 848. 18E+18. KF=
148359. 848. 18E+18. KF=
149028. 848. 18E+18. KF=
149697. 848. 18E+18. KF=
150366. 848. 18E+18. KF=
151035. 848. 18E+18. KF=
151704. 848. 18E+18. KF=
152373. 848. 18E+18. KF=
153042. 848. 18E+18. KF=
153711. 848. 18E+18. KF=
154380. 848. 18E+18. KF=
155049. 848. 18E+18. KF=
155718. 848. 18E+18. KF=
156387. 848. 18E+18. KF=
157056. 848. 18E+18. KF=
157725. 848. 18E+18. KF=
158394. 848. 18E+18. KF=
159063. 848. 18E+18. KF=
159732. 848. 18E+18. KF=
160401. 848. 18E+18. KF=
161070. 848. 18E+18. KF=
161739. 848. 18E+18. KF=
162408. 848. 18E+18. KF=
163077. 848. 18E+18. KF=
163746. 848. 18E+18. KF=
164415. 848. 18E+18. KF=
165084. 848. 18E+18. KF=
165753. 848. 18E+18. KF=
166422. 848. 18E+18. KF=
167091. 848. 18E+18. KF=
167760. 848. 18E+18. KF=
168429. 848. 18E+18. KF=
169098. 848. 18E+18. KF=
169767. 848. 18E+18. KF=
170436. 848. 18E+18. KF=
171105. 848. 18E+18. KF=
171774. 848. 18E+18. KF=
172443. 848. 18E+18. KF=
173112. 848. 18E+18. KF=
173781. 848. 18E+18. KF=
174450. 848. 18E+18. KF=
175119. 848. 18E+18. KF=
175788. 848. 18E+18. KF=
176457. 848. 18E+18. KF=
177126. 848. 18E+18. KF=
177795. 848. 18E+18. KF=
178464. 848. 18E+18. KF=
179133. 848. 18E+18. KF=
179802. 848. 18E+18. KF=
180471. 848. 18E+18. KF=
181140. 848. 18E+18. KF=
181809. 848. 18E+18. KF=
182478. 848. 18E+18. KF=
183147. 848. 18E+18. KF=
183816. 848. 18E+18. KF=
184485. 848. 18E+18. KF=
185154. 848. 18E+18. KF=
185823. 848. 18E+18. KF=
186492. 848. 18E+18. KF=
187161. 848. 18E+18. KF=
187830. 848. 18E+18. KF=
188499. 848. 18E+18. KF=
189168. 848. 18E+18. KF=
189837. 848. 18E+18. KF=
190506. 848. 18E+18. KF=
191175. 848. 18E+18. KF=
191844. 848. 18E+18. KF=
192513. 848. 18E+18. KF=
193182. 848. 18E+18. KF=
193851. 848. 18E+18. KF=
194520. 848. 18E+18. KF=
195189. 848. 18E+18. KF=
195858. 848. 18E+18. KF=
196527. 848. 18E+18. KF=
197196. 848. 18E+18. KF=
197865. 848. 18E+18. KF=
198534. 848. 18E+18. KF=
199203. 848. 18E+18. KF=
199872. 848. 18E+18. KF=
200541. 848. 18E+18. KF=
201210. 848. 18E+18. KF=
201879. 848. 18E+18. KF=
202548. 848. 18E+18. KF=
203217. 848. 18E+18. KF=
203886. 848. 18E+18. KF=
204555. 848. 18E+18. KF=
205224. 848. 18E+18. KF=
205893. 848. 18E+18. KF=
206562. 848. 18E+18. KF=
207231. 848. 18E+18. KF=
207900. 848. 18E+18. KF=
208569. 848. 18E+18. KF=
209238. 848. 18E+18. KF=
209907. 848. 18E+18. KF=
210576. 848. 18E+18. KF=
211245. 848. 18E+18. KF=
211914. 848. 18E+18. KF=
212583. 848. 18E+18. KF=
213252. 848. 18E+18. KF=
213921. 848. 18E+18. KF=
214590. 848. 18E+18. KF=
215259. 848. 18E+18. KF=
215928. 848. 18E+18. KF=
216597. 848. 18E+18. KF=
217266. 848. 18E+18. KF=
217935. 848. 18E+18. KF=
218604. 848. 18E+18. KF=
219273. 848. 18E+18. KF=
219942. 848. 18E+18. KF=
220611. 848. 18E+18. KF=
221280. 848. 18E+18. KF=
221949. 848. 18E+18. KF=
222618. 848. 18E+18. KF=
223287. 848. 18E+18. KF=
223956. 848. 18E+18. KF=
224625. 848. 18E+18. KF=
225294. 848. 18E+18. KF=
225963. 848. 18E+18. KF=
226632. 848. 18E+18. KF=
227301. 848. 18E+18. KF=
227970. 848. 18E+18. KF=
228639. 848. 18E+18. KF=
229308. 848. 18E+18. KF=
229977. 848. 18E+18. KF=
230646. 848. 18E+18. KF=
231315. 848. 18E+18. KF=
231984. 848. 18E+18. KF=
232653. 848. 18E+18. KF=
233322. 848. 18E+18. KF=
233991. 848. 18E+18. KF=
234660. 848. 18E+18. KF=
235329. 848. 18E+18. KF=
235998. 848. 18E+18. KF=
236667. 848. 18E+18. KF=
237336. 848. 18E+18. KF=
238005. 848. 18E+18. KF=
238674. 848. 18E+18. KF=
239343. 848. 18E+18. KF=
240012. 848. 18E+18. KF=
240681. 848. 18E+18. KF=
241350. 848. 18E+18. KF=
242019. 848. 18E+18. KF=
242688. 848. 18E+18. KF=
243357. 848. 18E+18. KF=
244026. 848. 18E+18. KF=
244695. 848. 18E+18. KF=
245364. 848. 18E+18. KF=
246033. 848. 18E+18. KF=
246702. 848. 18E+18. KF=
247371. 848. 18E+18. KF=
248040. 848. 18E+18. KF=
248709. 848. 18E+18. KF=
249378. 848. 18E+18. KF=
250047. 848. 18E+18. KF=
250716. 848. 18E+18. KF=
251385. 848. 18E+18. KF=
252054. 848. 18E+18. KF=
252723. 848. 18E+18. KF=
253392. 848. 18E+18. KF=
254061. 848. 18E+18. KF=
254730. 848. 18E+18. KF=
255399. 848. 18E+18. KF=
256068. 848. 18E+18. KF=
256737. 848. 18E+18. KF=
257406. 848. 18E+18. KF=
258075. 848. 18E+18. KF=
258744. 848. 18E+18. KF=
259413. 848. 18E+18. KF=
260082. 848. 18E+18. KF=
260751. 848. 18E+18. KF=
261420. 848. 18E+18. KF=
262089. 848. 18E+18. KF=
262758. 848. 18E+18. KF=
263427. 848. 18E+18. KF=
264096. 848. 18E+18. KF=
264765. 848. 18E+18. KF=
265434. 848. 18E+18. KF=
266103. 848. 18E+18. KF=
266772. 848. 18E+18. KF=
267441. 848. 18E+18. KF=
268110. 848. 18E+18. KF=
268779. 848. 18E+18. KF=
269448. 848. 18E+18. KF=
270117. 848. 18E+18. KF=
270786. 848. 18E+18. KF=
271455. 848. 18E+18. KF=
272124. 848. 18E+18. KF=
272793. 848. 18E+18. KF=
273462. 848. 18E+18. KF=
274131. 848. 18E+18. KF=
274800. 848. 18E+18. KF=
275469. 848. 18E+18. KF=
276138. 848. 18E+18. KF=
276807. 848. 18E+18. KF=
277476. 848. 18E+18. KF=
278145. 848. 18E+18. KF=
278814. 848. 18E+18. KF=
279483. 848. 18E+18. KF=
280152. 848. 18E+18. KF=
280821. 848. 18E+18. KF=
281490. 848. 18E+18. KF=
282159. 848. 18E+18. KF=
282828. 848. 18E+18. KF=
283497. 848. 18E+18. KF=
284166. 848. 18E+18. KF=
284835. 848. 18E+18. KF=
285504. 848. 18E+18. KF=
286173. 848. 18E+18. KF=
286842. 848. 18E+18. KF=
287511. 848. 18E+18. KF=
288180. 848. 18E+18. KF=
288849. 848. 18E+18. KF=
289518. 848. 18E+18. KF=
290187. 848. 18E+18. KF=
290856. 848. 18E+18. KF=
291525. 848. 18E+18. KF=
292194. 848. 18E+18. KF=
292863. 848. 18E+18. KF=
293532. 848. 18E+18. KF=
294201. 848. 18E+18. KF=
294870. 848. 18E+18. KF=
295539. 848. 18E+18. KF=
296208. 848. 18E+18. KF=
296877. 848. 18E+18. KF=
297546. 848. 18E+18. KF=
298215. 848. 18E+18. KF=
298884. 848. 18E+18. KF=
299553. 848. 18E+18. KF=
300222. 848. 18E+18. KF=
300891. 848. 18E+18. KF=
301560. 848. 18E+18. KF=
302229. 848. 18E+18. KF=
302898. 848. 18E+18. KF=
303567. 848. 18E+18. KF=
304236. 848. 18E+18. KF=
304905. 848. 18E+18. KF=
305574. 848. 18E+18. KF=
306243. 848. 18E+18. KF=
306912. 848. 18E+18. KF=
307581. 848. 18E+18. KF=
308250. 848. 18E+18. KF=
308919. 848. 18E+18. KF=
309588. 848. 18E+18. KF=
310257. 848. 18E+18. KF=
310926. 848. 18E+18. KF=
311595. 848. 18E+18. KF=
312264. 848. 18E+18. KF=
312933. 848. 18E+18. KF=
313602. 848. 18E+18. KF=
314271. 848. 18E+18. KF=
314940. 848. 18E+18. KF=
315609. 848. 18E+18. KF=
316278. 848. 18E+18. KF=
316947. 848. 18E+18. KF=
317616. 848. 18E+18. KF=
318285. 848. 18E+18. KF=
318954. 848. 18E+18. KF=
319623. 848. 18E+18. KF=
320292. 848. 18E+18. KF=
320961. 848. 18E+18. KF=
321630. 848. 18E+18. KF=
322299. 848. 18E+18. KF=
322968. 848. 18E+18. KF=
323637. 848. 18E+18. KF=
324306. 848. 18E+18. KF=
324975. 848. 18E+18. KF=
325644. 848. 18E+18. KF=
326313. 848. 18E+18. KF=
326982. 848. 18E+18. KF=
327651.

[illegible]

[illegible]

APPENDIX B

GAIN AND ABSORPTION COEFFICIENTS

The following are the gain and absorption coefficients at line center for Doppler and pressure broadening with ω in cm^{-1} units.

GAIN COEFFICIENT

$$g(\omega) = \frac{h B_{1 \rightarrow u}}{4\pi} \omega_{u1} \phi(\omega - \omega_c) \left(\frac{g_l}{g_u} N_u - N_l \right) \quad (1)$$

$$B_{lu} = \frac{1}{2hc\omega_{u1}} A_{ul} \frac{g_u}{g_l} \quad (2)$$

$$\phi(\omega, \nu, J, m) = \left(\frac{\ln 2}{\pi} \right)^{1/2} \frac{1}{\Delta\nu_{DP}(\nu, J, m)} K(x, y) \quad (3)$$

$$\lambda_{u1} = \frac{1}{\omega_{u1}} \quad (4)$$

$$\Delta\nu_{DP} = \left(\frac{2k \ln 2}{c} \right)^{1/2} \left(\frac{T}{M} \right)^{1/2} \omega_{u1} = 3.58 \times 10^{-7} \left(\frac{T}{M} \right)^{1/2} \omega_{u1} \quad (5)$$

$$\Delta\nu_{LR} = T^{-1/2} \left[\sum_i p_i \alpha_i \right] \quad (5')$$

$$\alpha_1 = T^{1/2} \left(\frac{\gamma}{p} \right) \quad (5')$$

$$g(\omega) = \frac{1}{8\pi} \lambda_{u1}^2 A_{u1} \frac{g_u}{g_l} \frac{1}{\Delta\nu_{DP}} \sqrt{\frac{\ln 2}{\pi}} K(x, y) \left(\frac{g_l}{g_u} \frac{N_u - N_l}{g_u} \right) \quad (6)$$

$$x = (\ln 2)^{1/2} \frac{|\omega - \omega_c(v, J, m)|}{\Delta\nu_{DP}(v, J, m)} \quad (7)$$

$$y = (\ln 2)^{1/2} \frac{\Delta\nu_{LR}(v, J)}{\Delta\nu_{DP}(v, J, m)} \quad (8)$$

AT LINE CENTER

$$\omega = \omega_c \text{ and } x = 0 \quad (9)$$

VOIGT FUNCTION IS DEFINED AS

$$K(0, y) = \left[1 - \operatorname{erf}(y) \right] \exp(y^2) \quad (10)$$

DOPPLER BROADENING

$$y = 0 \quad K(0, 0) = 1 \quad (11)$$

$$\phi_{DP}(\omega_c) = (\ln 2 / \pi)^{1/2} / (\Delta\nu)_{DP} \quad (12)$$

LORENTZ BROADENING

$$y \div = K(0, y) \div 1/(\pi^{1/2} y) \quad (13)$$

$$\phi_{LR}(\omega_c) = \frac{1}{\pi(\Delta\nu)_{LR}} \quad (14)$$

ABSORPTION COEFFICIENT

$$k_\nu = g(\omega) \quad (15)$$

$$k_\nu = \frac{1}{8\pi} \lambda_{u1}^2 A_{u1} \frac{g_u}{g_l} \frac{1}{(\Delta\nu)_{DP}} \frac{1}{c} \sqrt{\frac{\ln 2}{\pi}} K(x, y) N_1 \left(1 - \frac{g_l}{g_u} \frac{N_u}{N_l}\right) \quad (16)$$

$$k_\nu = \sigma_s N_1 \left(1 - \frac{g_l}{g_u} \frac{N_u}{N_l}\right) \quad (17)$$

$$\sigma_s = \frac{1}{8\pi} \lambda_{u1}^2 A_{u1} \frac{g_u}{g_l} \frac{1}{(\Delta\nu)_{DP}} \frac{1}{c} \sqrt{\frac{\ln 2}{\pi}} K(x, y) \quad (18)$$

$$\left(\frac{dn_1}{dt}\right)_{ph} = c_1 \frac{z_1 I(t)}{\rho} \left[1 - \exp \left[-z_2 \rho \left(\frac{n_1}{g_1} - \frac{n_u}{g_u} \right) \right] \right] \quad (19)$$

$$z_2 = k_v I N_A \quad z_2 = \sigma_s I g_1 N_A \left[\frac{n_1}{g_1} - \frac{n_u}{g_u} \right] \quad (20)$$

$$z_2' = j_s I g_1 N_A \quad (21)$$

LABORATORY OPERATIONS

The Laboratory Operations of The Aerospace Corporation is conducting experimental and theoretical investigations necessary for the evaluation and application of scientific advances to new military space systems. Versatility and flexibility have been developed to a high degree by the laboratory personnel in dealing with the many problems encountered in the nation's rapidly developing space systems. Expertise in the latest scientific developments is vital to the accomplishment of tasks related to these problems. The laboratories that contribute to this research are:

Aerophysics Laboratory: Launch vehicle and reentry aerodynamics and heat transfer, propulsion chemistry and fluid mechanics, structural mechanics, flight dynamics; high-temperature thermomechanics, gas kinetics and radiation; research in environmental chemistry and contamination; cw and pulsed chemical laser development including chemical kinetics, spectroscopy, optical resonators and beam pointing, atmospheric propagation, laser effects and countermeasures.

Chemistry and Physics Laboratory: Atmospheric chemical reactions, atmospheric optics, light scattering, state-specific chemical reactions and radiation transport in rocket plumes, applied laser spectroscopy, laser chemistry, battery electrochemistry, space vacuum and radiation effects on materials, lubrication and surface phenomena, thermionic emission, photosensitive materials and detectors, atomic frequency standards, and bioenvironmental research and monitoring.

Electronics Research Laboratory: Microelectronics, GaAs low-noise and power devices, semiconductor lasers, electromagnetic and optical propagation phenomena, quantum electronics, laser communications, lidar, and electro-optics; communication sciences, applied electronics, semiconductor crystal and device physics, radiometric imaging; millimeter-wave and microwave technology.

Information Sciences Research Office: Program verification, program translation, performance-sensitive system design, distributed architectures for spaceborne computers, fault-tolerant computer systems, artificial intelligence, and microelectronics applications.

Materials Sciences Laboratory: Development of new materials: metal matrix composites, polymers, and new forms of carbon; component failure analysis and reliability; fracture mechanics and stress corrosion; evaluation of materials in space environment; materials performance in space transportation systems; analysis of systems vulnerability and survivability in enemy-induced environments.

Space Sciences Laboratory: Atmospheric and ionospheric physics, radiation from the atmosphere, density and composition of the upper atmosphere, aurorae and airglow; magnetospheric physics, cosmic rays, generation and propagation of plasma waves in the magnetosphere; solar physics, infrared astronomy; the effects of nuclear explosions, magnetic storms, and solar activity on the earth's atmosphere, ionosphere, and magnetosphere; the effects of optical, electromagnetic, and particulate radiations in space on space systems.